TECHNISCHE UNIVERSITÄT WIEN
Vienna | Austria

Master Thesis

Bringing osteogenic activity to MC3T3-E1-loaded microscaffolds

carried out for the purpose of obtaining the degree of Master of Science (MSc or Dipl.-Ing. or DI), submitted at TU Wien, Faculty of Mechanical and Industrial Engineering, by

Federico Pugliese

Mat.Nr.: 12122515

under the supervision of

Univ.Prof. Dr.rer.nat Aleksandr Ovsianikov

and Univ. Ass. Dr. Olivier Guillaume

and Projektass. (FWF) Dipl.-Ing. Stephan Schandl

and Projektass. Dipl.-Ing. Kopinski-Grünwald Oliver

Institute of Materials Science and Technology

Research Unit of Polymers and Composites

Research Group for 3D Printing and Biofabrication

Vienna, March 2024

Abstract

Bone-related pathologies and injuries represent a complex matter of study due to the major limitations of tissue self-healing and the diverse factors into play. When treating large defects, above the critical size, the native repair process results to be insufficient and the incorporation of engineered materials and devices is fundamental to achieve a full recovery. In this context, regenerative medicine plays a pivotal role in the development and evaluation of new solutions, allowing to address a wider range of cases and conditions. Novel approaches aim to exploit and merge stem cell differentiation with diverse stimulating agents, whether synthetically or naturally-derived. Autografts are currently considered the gold-standard procedure in this field. The graft provides osteogenic and osteoinductive cues alongside stem cells while restoring the mechanical and biological properties of the damaged tissue. However, limiting factors in their application are high surgical costs and times, and an increased risk of comorbidities at the donor site. Scaffold-based strategies are preferred as alternative option due to the possibility to tune the device characteristics to the intended use and gain better control on different aspects of the procedure. A broad range of biocompatible materials can be examined to support cell expansion and differentiation, also allowing to incorporate further factors in the final construct. BMP-2 is one of the most frequently examined osteogenic factors in bone regeneration, alongside ceramic compounds resembling the native tissue composition and properties.

In the current study, a recently developed microscaffold was utilised to guide and sustain cell culture. The main purpose was to gain better insight into the achievable differentiation with the combination of diverse factors. MC3T3-E1 cells have been selected for their capability to differentiate into osteoblasts when exposed to BMP-2. This latter aspect has been tested and confirmed in 2D culture first, measuring the promoted extracellular mineralization via Alizarin Red S (ARS) staining. Afterwards, a three-dimensional setup was designed with the involvement of a fullerene-shaped microscaffold, named buckyball (BB), able to shield cellular aggregates from mechanical damages and allow for the integration of other cues, such as calcium microparticles and BMP-2. Their inclusion was expected to promote major osteodifferentiation in respect of standard culture conditions. Samples were analysed with ARS and Calcein Green staining, and qPCR over a 14-days culture period. BMP-2 was proven to trigger a higher calcium deposition, similarly to the 2D case. Furthermore, the combination of BMP-2 and calcium microparticles seemed to accelerate the differentiation process, with osteogenic markers' overexpression and matrix remodelling taking place after only one week of culture. However, the control groups also showed minor mineral content and gene upregulation, suggesting that the passage to three-dimensional conditions could have been sufficient to trigger some differentiation. The MC3T3-E1 cell line was thus considered suitable for testing growth-factors-functionalized microscaffolds for regenerative solutions in bone repair, opening up to further applications to find the most effective combination of osteogenic factors to achieve a greater regenerative potential.

Keywords: MC3T3-E1, BMP-2, calcium-phosphate particles, buckyball, microscaffold

Acknowledgement

I would like to use this opportunity to express my gratitude to the people who contributed to this work with their expertise, support and guidance.

First and foremost, I would like to thank Univ.Prof. Dr.rer.nat Aleksandr Ovsianikov and Univ. Ass. Dr. Olivier Guillaume for giving me the opportunity to work on such an interesting project and topic. Working and getting to know such an interdisciplinary and heterogeneous group represented the most stimulating part of this experience.
I want to thank Marica Markovic for introducing me to cell culture and welcoming me into the group in the very first place, being always available for everyone inside and outside the lab.

Furthermore, I want to thank Projektass. (FWF) Dipl.-Ing. Stephan Schandl and Projektass. Dipl.-Ing. Kopinski-Grünwald Oliver for supervising and reviewing all my work, clarifying my doubts and walking me through most of the techniques I learned. I would like to express my gratitude also to Univ.Ass.In PhD Julia Fernández Pérez for the constant support and advice throughout my whole experience in the group. My special thanks go to my colleagues at the Research Group for 3D Printing and Biofabrication, for making me feel welcome in the group from day one and for being there not only in the lab moments but most importantly in those outside of it.

Lastly, I want to thank my family for supporting and encouraging me throughout my studies and, most of all, my life in Vienna.

Table of Contents

1 Introduction 7
2 Objective and Approach 9
3 Theoretical Background 11
3.1 MC3T3-E1 11
3.2 Scaffold 11
3.2.1 Scaffold Design 13
3.3 BMP-2 14
3.4 Calcium-based Biomaterials 15
3.5 Analysis of Osteogenic Differentiation 16
3.5.1 qPCR 16
3.5.2 Alizarin Red S Staining 17
3.6 ELISA 18
4 Materials and Methods 19
4.1 Ceramic Powder 19
4.1.1 Powder Preparation 19
4.2 Scaffold 19
4.2.1 Aminolysis 19
4.2.2 Heparin Coupling 20
4.3 BMP-2 Loading and Elution 20
4.3.1 Buckyballs 20
4.3.2 Ceramic Powder 20
4.3.3 ELISA Protocol 21
4.4 MC3T3-E1 Culture 21
4.4.1 2D Differentiation 21
4.4.2 Plate Coating 22
4.4.3 3D Differentiation 22
4.4 Alizarin Red S Staining 23
4.5 Calcein Green Staining 24
4.6 Polymerase Chain Reaction 24
4.6.1 RNA Isolation 24
4.6.2 cDNA Synthesis 25

4.6.3 qPCR with SSoAdvanced SYBR Green Supermix 25
5 Results 27
5.1 Ceramic Powder 27
5.1.2 BMP-2 Release Study 27
5.2 Scaffold 28
5.2.1 Surface Modification 28
5.2.2 BMP-2 Loading and Elution 28
5.3 MC3T3-E1 Culture 29
5.3.1 2D Differentiation 29
5.4 3D Differentiation 30
5.4.1 Alizarin Red S Staining 31
5.4.2 Calcein Green Staining 32
5.4.3 Polymerase Chain Reaction 34
6 Discussion 35
7 Conclusion and Outlook 37
Bibliography 38

1 Introduction

Bone tissue undergoes continuous remodelling and is characterized by a significant self-healing potential. However, extensive damages and defects, larger than the critical size of 2 cm [1], e.g. resulting from tumour resections, and genetic or autoimmune pathologies, cannot be repaired by the native tissue without an external intervention. Therefore, these latter cases represent a challenging matter of research [2], [3]. When developing adequate therapeutical strategies for clinical practice, a broad range of factors and considerations comes into play and significantly affects the success of such procedures.

In the field of tissue engineering and regenerative medicine (TERM), several approaches to address extensive tissue defects or deficiencies are available and allow for the study of diverse applications in patients' treatment. When referring specifically to bone-related pathologies, the gold standard is represented by autografts [4], [5]. Such a procedure guarantees a combination of osteogenic (due to the presence of native stem cells), osteoinductive (growth factors), and osteoconductive (mineral content) effects promoting repair via the activation of a set of regenerative processes. Moreover, the use of bone grafts would naturally maintain and replicate the native tissue's biological and mechanical properties. However, limiting factors such as the risk of additional morbidities at the donor site, the shortage and immunogenic complications in alternative allografts and xenografts, and increased surgical costs and times highly impact the possible applications in common practice [3], [5], [6], [7].

Therefore, further options are explored in research interconnecting diverse fields. Comparable or even better results can indeed be obtained when combining the beneficial effects of stem cells, biomaterials and osteoinductive/conductive cues [2], [3], [4], [8]. Many factors are to be taken into consideration, starting from the selection of the most suitable lineage for the intended use.

In the case of bone regeneration, various cell lineages are available, ranging from pluripotent bone marrow or adipose-derived mesenchymal stem cells (BM-MSC [9], ASCs [10], [11]) to more specialised myoblast (i.e. C2C12) or preosteoblast (i.e. MC3T3-E1) lineages [12]. They all share the capability to differentiate into osteoblasts when stimulated with specific media, growth factors and/or osteoinductive compounds. Thus, new variables are involved, depending on the presence of synthetic and/or biological compounds providing support for cell growth and triggering a stronger response.

The first step is a modification of the culturing conditions, which significantly influences the outcomes of cell differentiation. The differentiation into osteoblasts is typically obtained with the addition of osteogenic growth factors in the culture medium, in most cases ascorbic acid 2-phosphate (AA2P) and glycerophosphate, and possibly including vitamin D3 and dexamethasone depending on the targeted cell lineage [10], [12]. Moreover, low-binding culture surfaces can be introduced to form spheroids and obtain 3D constructs, rather than two-dimensional monolayers. This is intended to better replicate physiological conditions and is demonstrated to promote a major expression of growth factors increasing the tissue healing and anti-inflammatory properties [13], [14].

Many studies available in the literature have investigated the possibility of including calcium-based compounds as substrate, scaffold, or stimulating agent in cell culture, both in 2D and in spheroids. Such studies demonstrated the osteoconductive potential of these materials, producing a stronger cells' stimulation and consequent differentiation [7], in terms of osteogenic marker expression and

mineral deposition. They employed diverse ceramic compounds with different sizes and structures, e.g. hydroxyapatite (HA) [15], tricalcium [16], [17] or biphasic calcium phosphate [6] among others, as well as multiple cell lines. The common thread is the introduction of ceramic composites mimicking bone tissue composition and properties and promoting a cell response similar to physiological conditions. They can be designed to reproduce the biodegradability, bioactivity, and grain morphology of natural bone [7]. Therefore, the incorporation of calcium particles could provide various beneficial effects and improve the final outcomes of stem cell-based treatments.

Despite the listed advantages, ceramic-based materials do not show osteoinductive properties, which typically stimulate the treated tissue to start the regenerative process and repair itself. To address this issue, ceramic particles can be used for surface adsorption and later release of other osteogenic cues.

This is the case with bone morphogenic proteins (BMPs), a group of potent growth factors capable of directly inducing the differentiation of targeted cells into osteoblasts [18]. In the context of bone repair, BMP-2 represents the most frequently chosen and analysed one, capable of stimulating diverse cell lineages, such as ASCs [19], BM-MSCs [20], or MC3T3-E1 [12], [21] among others. Due to its strong effects on cell differentiation, several studies aim to obtain a more stable and prolonged administration compared to the standard inclusion in solution. The most popular choices are calcium composites [3], [22], or synthetically-derived materials [23] as support systems for binding and controlled delivery.

A further distinction can then be made between scaffold-free and scaffold-based solutions. As previously described, the former approach involving spheroids' formation overcomes the limitations of monolayer cultures, enhancing cell-cell and cell-matrix interactions. It also presents advantages in therapeutical applications when compared to monodispersed cell suspensions. Such three-dimensional structures are recognized to improve survival and retention of the differentiated phenotype and cells in the target site [14], [24], [25]. In addition, single spheroids can be fused to obtain larger aggregates via a bottom-up self-assembly process and allowing to adapt them to a broader range of size and shape defects [26]. This is particularly relevant and offers new possibilities in the development of case-specific treatments.

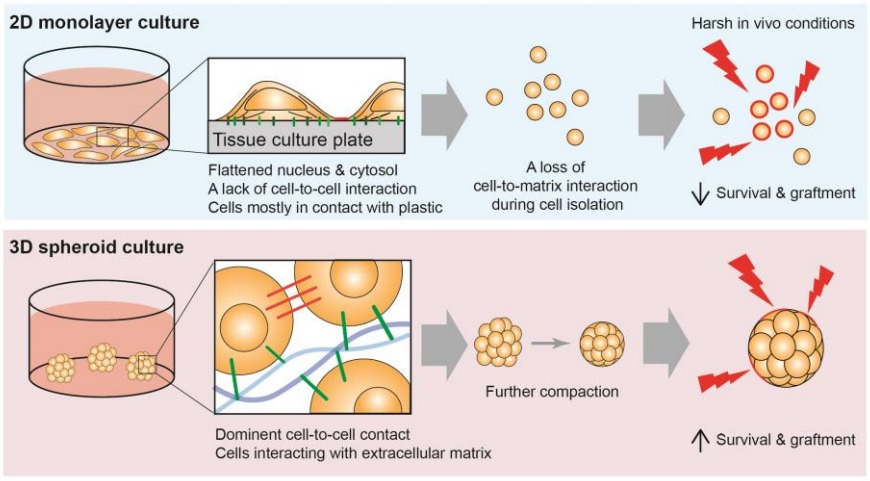

Figure 1: 2D and 3D culture comparison. Adapted from [25].

Such aspects can be enhanced even further with the introduction of polymeric scaffolds, varying in composition, properties, and size. For such reasons, several materials are being investigated in

research to gain better control on spheroids' formation while improving the overall outcomes of tissue repair. Various solutions are studied, ranging from hydrogel embedding of cells [14] to natural or synthetic fibres and particles [25], aiming to reproduce the mechanical and biological stimuli characterizing the native structure. A similar approach is intended to sustain matrix deposition and cell proliferation while the newly formed tissue gradually substitutes or integrates the bioactive implant. Furthermore, the presence of scaffolds can offer mechanical protection and the possibility to control the geometry of cells' aggregates [27]. Thus, the current study focused on the integration of micro-scale porous constructs in culture, merging the advantages of both approaches, scaffold-free and scaffold-based. The characteristic high porosity is necessary to allow spheroids' formation and growth at the core, while the external shell determines their final shape. Moreover, such designed scaffolds can be combined with other stimulating agents in different ways, whether incorporating them on the material itself or within the spheroids. This opens up a new set of possible approaches and solutions still to be fully explored, merging the characteristics and properties of cell-based and scaffold-based approaches. The "third strategy for TERM" hence aims to exploit the major advantages of both techniques and their combination, integrating single spheroids in robust, porous microscaffolds [27].

2 Objective and Approach

Similar results have been demonstrated with a recently developed 2PP-printed microscaffold design (called buckyball, BB [27]), replicating the architecture of C60 fullerene. The highly porous cage-like structure allows cells to aggregate at the core without interfering in their maturation and differentiation. Their self-assembly properties are preserved, and a major control on the final size can be achieved due to the lower overall compaction. For these reasons, the same microscaffold is used in the present study. As previously described, the introduction of such microscaffolds stabilizes spheroids formation, encapsulating and confining them while providing protection. The cell number and viability over time are thus significantly improved when compared to monodispersed suspensions or single spheroids [27].

Finding the right balance and combination of the investigated factors is one of the most challenging aspects of regenerative medicine. In this study, a potential hybrid technique is presented and analysed, aiming to enhance the osteogenicity of scaffolded spheroids for future applications in bone repair. Different tools were merged to exploit the respective advantages and account for the deficiencies of cellular spheroids alone.

The therapeutical potential of this hybrid approach relies on the intrinsic osteogenicity of the scaffolded spheroids. In this context, the use of scaffolds presents two further advantages: a reduced and more controlled cellular compaction over time, preventing the insurgence of hypoxic conditions at the core, and the possibility to integrate further osteoinductive factors to enhance cellular stimulation, by inclusion in the spheroids' formation.

Thus, the addition of ceramic-based compounds (i.e. micro-sized calcium phosphate particles) was investigated in two conditions, namely with or without the further adsorption of BMP-2 onto powder particles, to merge the osteogenic potential of both factors.

Contrarily to Guillaume et al. [27], where human immortalized ASCs were used, a different cell type was selected for the present study, namely MC3T3-E1, a murine preosteoblast lineage. In the literature, it demonstrated to strongly respond to BMP-2 [28], [29] and calcium-based materials [6].

The main purposes here were to firstly confirm the effects of BMP-2 on MC3T3-E1 cells in 2D conditions, then to evaluate the differentiation ability and the effects of BMP-2 and/or CaP microparticles, whether BMP-2-laden or not, in scaffolded spheroids culture.

3 Theoretical Background

3.1 MC3T3-E1

In TERM, most therapeutical strategies rely on the culture and differentiation of specific cell lineages to restore and enhance tissue repair. The selected cells are stimulated with culture media supplemented with growth factors, typically ascorbic acid 2-phosphate (AA2P) and glycerophosphate [11], [20], [21]. Their insertion at the injury site can trigger and achieve the complete repair of large defects, which would not be possible without intervention. The most frequently chosen lineages are human ASCs [10], [11], BM-MSCs [24], C2C12 [29], and MC3T3-E1 [21] among others. The latter cell line has been selected for this study to test the osteoinductive potential of the investigated factors, namely BMP-2 and a calcium-based ceramic powder, based on previous findings in the literature [6], [12], [29]. MC3T3-E1 cells, a murine-derived preosteoblast lineage, are frequently used to assess the osteogenicity of diverse approaches, varying in the media, biomaterials, and/or supplements [12], [28]. Studies focused on the treatment of degenerative pathologies or addressing the regeneration of large defects have been developed with the introduction of MC3T3-E1 for their characteristic feature to undergo differentiation into osteoblasts after a short culture period and to produce significant extracellular mineralization [21], [30]. More specifically, these cells demonstrated a strong response to the addition of BMP-2 in 2D culture with a dose-dependent behaviour and a gradually increasing osteogenic differentiation compared to standard conditions [29]. Similar results have been proven in spheroid culture, with MC3T3-E1 responding to the incorporation of BMP-2 and/or calcium particles in the aggregation process. Contrarily to monolayer culture, some minor differentiation was also detected in standard conditions, with markers upregulation and mineral deposition in samples fed with expansionmedium or osteogenic medium only [31], [32], [33]. Therefore, MC3T3-E1 are widely considered one of the most suitable options in the development and evaluation of therapeutical strategies addressing bone defects and related pathologies.

3.2 Scaffold

The design and incorporation of scaffolds in cell culture allow to overcome the deficiencies and limits of a cell-based approach. The injection of spheroids in suspension at the injury site presents some major disadvantages in the long term, with a progressively decreasing cell number and viability, significantly impacting the final success of the procedure [27]. Therefore, scaffolds are developed to assist cell aggregation and expansion, providing better control of the final shape and size of the cellular construct, with reduced compaction over time [25]. Cell retention and survival are also significantly improved [14]. Several options are available in terms of size, shape, and material, allowing to address a wide range of cases and obtain the desired properties and behaviour [4]. The developed strategy is supposed to allow cell attachment and proliferation, the integration of further compounds and factors to enhance differentiation, and to support the overall restoration of the targeted tissue. In this context, the combination of cellular spheroids, biomaterials and further osteogenic cues is meant to resemble the physicochemical environment of the *in vivo* tissue and thus produce a more physiological condition for regeneration.

A recently developed microscaffold is introduced for the culture of cell spheroids in three-dimensional conditions and the delivery of the investigated bioactive components (BMP-2 and calcium particles). The material is synthesized starting from a poly-ε-caprolactone (PCL) backbone, with the addition of urethane groups. PCL is widely used in scaffold-based approaches for regenerative treatments due to its low processing costs, superior mechanical properties (high strength and toughness at body temperature), and the wide range of chemical modifications available [8]. As an aliphatic polyester, it also shows biocompatibility and biodegradability, leading to the development of resorbable applications in wound dressing, drug delivery or suture [27], [34]. Moreover, the longer degradation time makes it a suitable solution for the integration and repair of hard, load-bearing tissues. Such characteristics allow to produce devices with a degradation kinetic that can be adjusted to match the deposition and formation of new tissue at the implantation site, with a gradual substitution of the implanted device [8].

In the case of buckyballs, a 2-step modification is performed on the PCL diol to synthesize a hexa-acrylate end-capped urethane-based PCL (UPCL-6). This step is meant to significantly enhance the crosslinking capacity of the molecule, so to access more complex structures and networks [34]. The obtained molecular structure is also able to combine and improve the overall properties of the incorporated moieties, such as the hardness of the polyacrylate ends and the softer PCL backbone, producing a final material with enhanced toughness and stiffness.

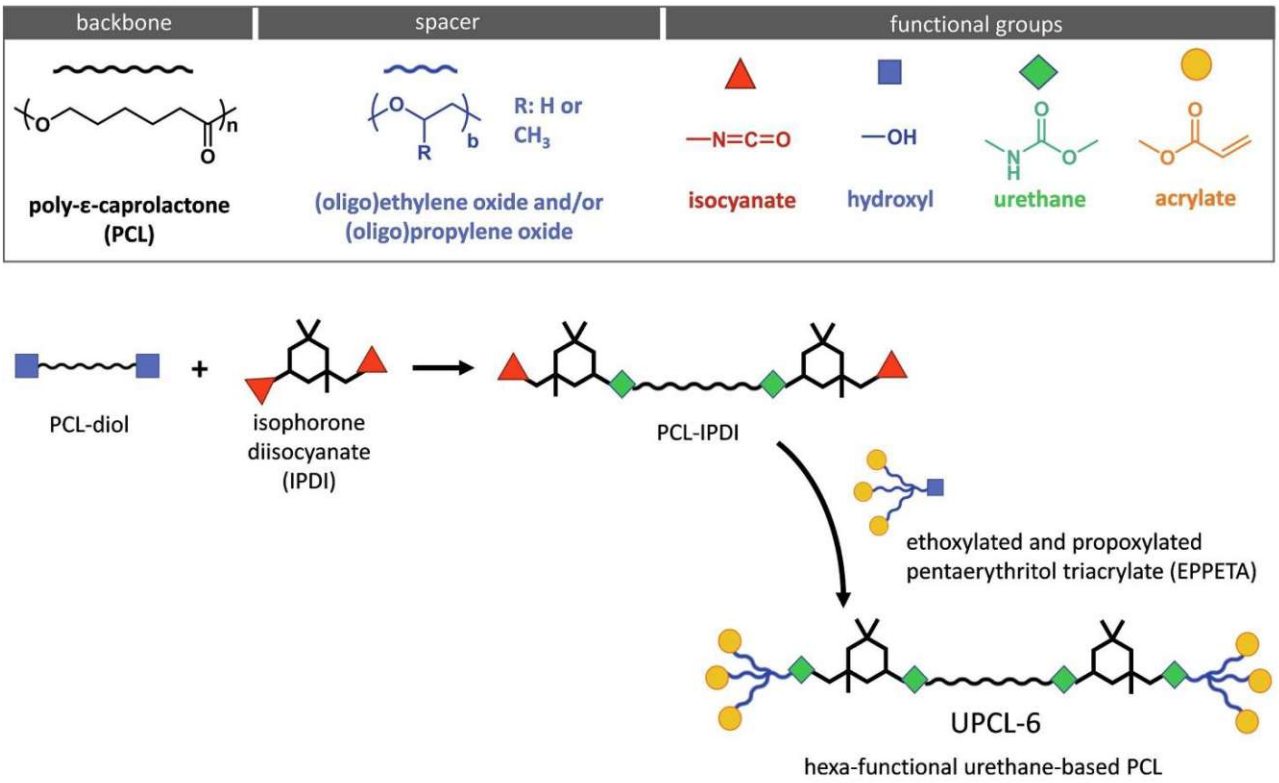

Figure 2: Two-step chemical modification of PCL to synthesize the final UPCL-6 molecule. Adapted from [34].

The displayed architecture also plays a vital role in the microscaffold synthesis with two-photon polymerization (2PP). The incorporation of photo-crosslinkable acrylate groups at each end opens a broad set of applications in laser-based 3D-printing techniques (i.e. 2PP) and thus to the development of complex structures with high definition. The UPCL-6 composition allows to overcome major issues associated with 2PP scaffold production using other materials, such as

swelling and inadequate crosslinking kinetics, low spatial resolution and deformation during processing. These aspects become fundamental when a highly porous, open geometry is desired and necessary. Most of these features are addressed with the increased amount of end groups introduced via chemical modification: more cross-linking moieties produce a denser and stronger network, resulting in reduced deformation during synthesis and implantation [34]. On the other hand, the creation of complex architectures is accessible thanks to the printing technique itself. With 2PP, also known as multiphoton lithography, a spatial resolution of a few hundred nanometres can be achieved. The process is based on the simultaneous absorption of two photons emitted with a femtosecond laser at the site of polymerization, a non-linear process allowing to localize the deposition of light in the photosensitive material in a highly confined and controlled area. The resultant effect is the triggering of a radical chain polymerization producing a dense network of crosslinked material. To enhance the efficiency of the whole procedure, the utilized resin needs to provide sufficient chemical and physical stability and a fast crosslinking kinetic, characteristics accounted for with the selection of UPCL-6.

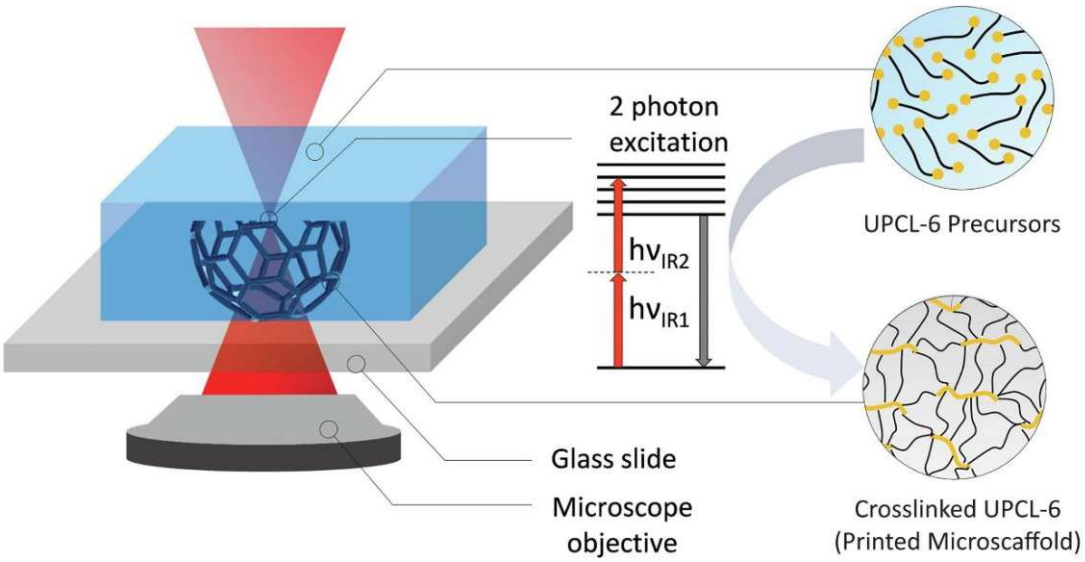

Figure 3: Simplified scheme showing 2PP functioning with UPCL-6-based scaffold production. Adapted from [34].

3.2.1 Scaffold Design

The characteristic highly porous design, based on the chemical structure of a fullerene molecule, is meant to allow cells' aggregation at the core while offering major control on the final shape and size and improving cell survivability. Another favouring factor is represented by the hydrophobicity of PCL, which prevents a fast cellular attachment on the scaffold struts and cell-cell interactions become predominant [27]. Porosity thus represents one of the key factors in the realization of an effective scaffold, not interfering with nutrient diffusion and cell migration. Moreover, the scaffold has a protective function, reducing the exposure of the encapsulated spheroid to mechanical damage (i.e. implantation site, mishandling). To overcome the major limitations of the printed scaffold, further chemical surface modification is necessary for safe and easier manipulation. Otherwise, such structures would clump in water complicating or impeding sorting, individual study, and transfer for later applications.

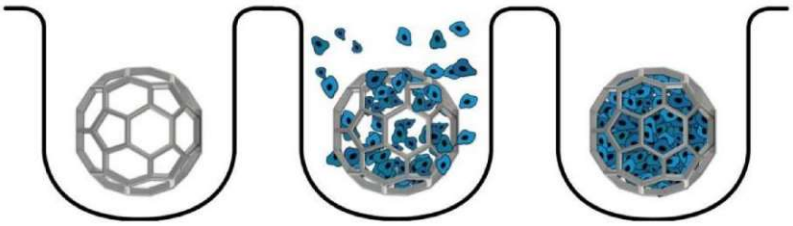

Figure 4: Cell seeding and aggregation in BBs. Adapted from [27].

Regarding its applications in cell culture, BBs have been shown not to interfere in spheroids' formation and differentiation [27]. The cellular aggregates are subjected to a decreased compaction over time, addressing and limiting the insurgence of hypoxic conditions at the core. A similar behaviour can be noticed when multiple spheroids are merged. The characteristic fusiogenic ability of cellular aggregates is also preserved, allowing for the creation of novel strategies based on the bottom-up self-assembly of multiple spheroids, and thus adaptable to various size defects. However, in the case of plain spheroids, a significant overall reduction of the construct size is detected over time, strongly deviating from the initial distribution and dimensions [26]. Therefore, a BB-based approach would allow to overcome the bottlenecks of cell-based strategies, with the possibility of developing a patient-specific therapy via the filling of the targeted defect with a sufficient amount of injectable BBs assembling in a stable tissue and promoting bone repair.

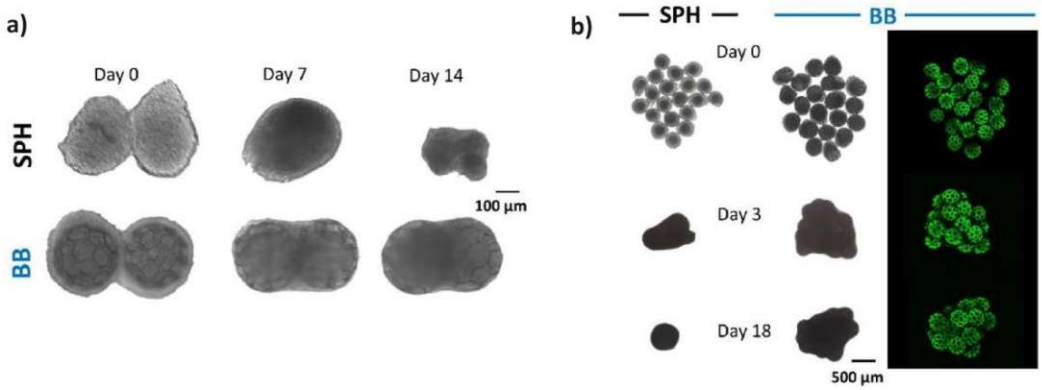

Figure 5: Comparison of compaction over time of a doublet (a) or 20 spheroids (b) without and with BB. Adapted from [27].

3.3 BMP-2

Bone morphogenic protein-2 (BMP-2) is an osteoinductive growth factor, composed of 396 amino acids, frequently introduced in cell culture to initiate osteodifferentiation and trigger ectopic mineralization. It was first identified in 1965 by Marshall R. Urist, after recognising its capability to trigger osteogenesis in extraskeletal tissues [35]. The potential insertion of BMP-2 in the regenerative treatment of large bone defects has been then explored in several animal studies. In physiological conditions, BMP-2 is a multifunctional molecule prevalently secreted by osteoblasts and belonging to the transforming growth factor β (TGF-β), involved in bone remodelling and homeostasis in adults. A loss in the osteogenic activity of BMP-2 was demonstrated to generate tissue dysfunctions such as osteopenia, bone fragility and spontaneous fracture or an osteoarthritis-like phenotype degenerating over time [36]. Moreover, the physiological decrease in BMP-2 expression occurring with age was recognized as one of the leading causes behind the progressive reduction of stem cell number and activity. An adequate secretion, or delivery in the case of

regenerative treatment, is thus fundamental for the maintenance and continuous renewal of bone tissue, preserving its mechanical and self-healing properties [36], [37]. It was noticed that in the absence of BMP-2 the initial tissue response to microfractures, wounds, and defects is not activated and minimal periosteal activity can be detected, impairing a spontaneous regeneration of the tissue. For these reasons, modification of polymeric or ceramic compounds with BMP-2 has been widely investigated for the development of stem cell-based and/or scaffold-based strategies able to restore and trigger the bone repair process [5], [6], [16], [22].
Regarding its functioning, BMP-2 initiates signal pathways playing a central role in the maturation stages of osteoblasts, binding to complexes of BMP type I and II receptors in the form of homo- or heterodimers. These pathways lead to the transcription of downstream genes, through the activation of SMAD-dependent processes mainly, but also the involvement of protein kinase A (PKA), and mitogen-activated protein kinase (MAPK) complexes [5], [36], [37].

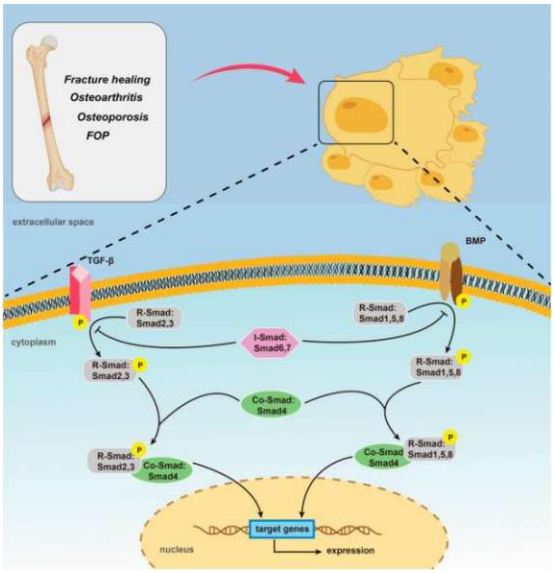

Figure 6: TGF-β and BMP-2/SMAD pathways triggering osteogenic genes expression.
Adapted from [37].

However, the supply of high dosages of BMP-2 can result in undesired side effects and complications, such as inflammation, fibrosis and heterotopic ossification [38]. The emergence of an inflammatory state highly impacts the efficacy of BMP-2 itself and provokes an increased osteoclastic activity, preventing a proper and complete regeneration of the bone defect. Low and mid-range concentrations are thus preferred in TERM applications, preserving the osteoinductive properties of the growth factor and offering a valid alternative to autograft-based therapies [5], [38].

3.4 Calcium-based Biomaterials

Among the various biomaterial solutions available for biomedical applications, ceramic-based materials are widely investigated for their osteoconductive properties. They are employed for the development of scaffolds, support devices, or additional factors in cell culture and differentiation [7], [17]. In particular, calcium phosphate-based compounds are studied for their capability to resemble the composition of native bone tissue and the physicochemical properties of its mineral content, resulting in a cellular stimulation similar to physiological conditions. The bioactivity and biocompatibility of CaP including solution are also exploited in the coating of other synthetic

implants. The result is an improved interaction with the tissues surrounding the implantation site and the promotion of bone ingrowth and integration of the device. Some limits are still to be considered. CaP biomaterials appear to be not suitable for large-scale structures, subjected to high load-bearing, due to their low fracture strength. Furthermore, they show minimal osteoinductive properties, highly impacting the formation of bone *de novo*. To improve this latter aspect, further modification is needed [7]. Despite the described issues, CaP-based solutions represent a valid substitute for autografts or allografts for the treatment of tissue defects. Diverse ceramic composites have been explored in the literature, ranging from hydroxyapatite (HA, [16], [22], to tricalcium phosphate (TCP, [17] A further application is recognized in the interaction of these biomaterials with proteins and growth factors, due to the strong affinity resulting in binding and adsorption. The most frequently examined interaction is with BMP-2, which can be loaded onto a CaP-based material for incorporation and delivery in cell culture [6], [15], [16], [22]. This latter solution would address two main complications specifically concerning 3D cultures. The aggregation and compaction of cells over longer periods of incubation lead in most cases to the emergence of hypoxic conditions in the core region of the spheroids since nutrients and oxygen cannot access it. This aspect significantly impacts the growth and survival of cells, affecting the success of the whole procedure. Hence, the incorporation of calcium particles in cellular constructs has been investigated in the present study to produce a looser structure and reduce compaction over time. Moreover, pre-loaded particles work as carrier substrates of potent factors such as BMP-2 or other nutrients, providing sustained and continuous stimulation to cells.

3.5 Analysis of Osteogenic Differentiation

Osteodifferentiation can be divided in three main stages: cell proliferation, ECM deposition and maturation, and matrix mineralization. A complex and broad set of growth factors, proteins, and osteoinductive compounds are secreted and involved in these different steps and in the formation of neo-tissue to repair the defect. The analysis of the achieved differentiation can be based on the characterization of the expressed proteins and markers involved in osteoblast activity, or the triggered extracellular mineral deposition, corresponding to the final stages of matrix and cellular maturation.

3.5.1 qPCR

The gold standard technique for gene expression evaluation is quantitative polymerase chain reaction, or qPCR, allowing to detect and quantify the expression of target sequences with high sensitivity and specificity. The foundations for the technique were first laid in 1985 with Mullis et al. work [39] and later implemented in the qPCR procedure by Higuchi [40].
As previously introduced, the set of secreted proteins and growth factors significantly varies throughout the different phases of differentiation. A further distinction can be made between early- and late-stage markers depending on the selected time span, responsible for diverse aspects of pre-osteoblasts and mature osteoblasts activity. The most commonly examined markers are alkaline phosphatase and collagen type 1 in the early phase, osteocalcin and osteopontin in the late stages of matrix maturation and mineralization, and Runx2 and osterix as regulators throughout the whole process [5], [31]. The quantification of these target sequences is typically determined in comparison to a standard gene, referred to as the housekeeping gene, which is expected to be stably expressed in

the cultured samples. Starting from the initially isolated RNA content, a first reverse transcription step is required to convert it to cDNA before proceeding with the amplification. A master mix is prepared including the obtained DNA strands, primers specific for the studied sequences, polymerase enzymes and deoxynucleoside triphosphates (dNTPs) for duplication. The qPCR process is composed of 30-45 cycles, alternating strand amplification and denaturation, monitoring the released fluorescence. The amplified DNA is labelled with fluorescent dyes, thus the resulting readout is directly dependent on the initial amount of cDNA isolated from the sample: the higher the initial number of molecules, the faster the signal increases. The subsequent analysis is based on the obtained quantitation cycle (C_q) values, indicating the cycle in which fluorescence surpassed the threshold value and thus could be detected. The sequences with a higher initial number of copies correspond to the lowest C_q readouts [41], [42].

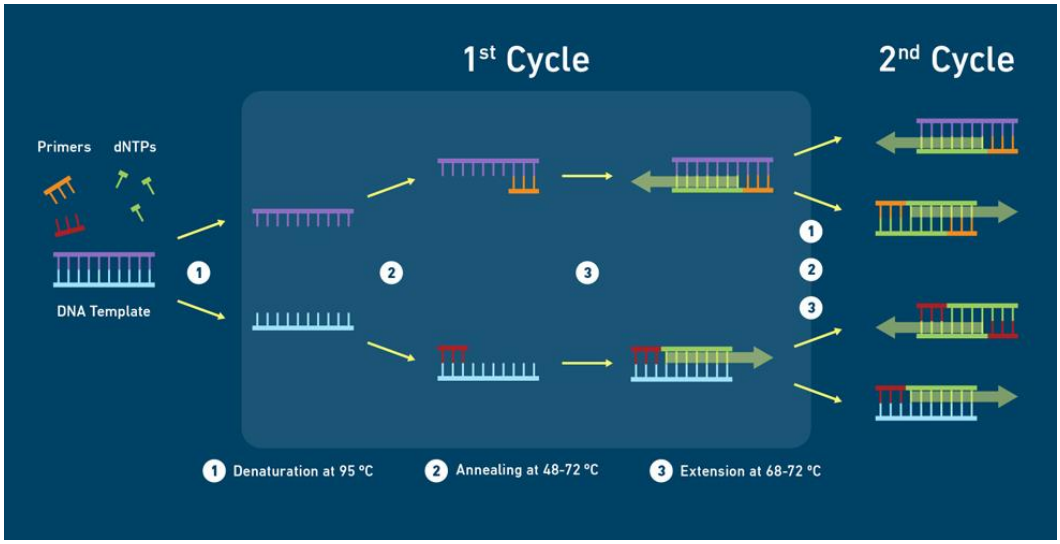

Figure 7: Simplified scheme for cDNA amplification cycles, with primer coupling to both strands to start duplication. Adapted from [41].

qPCR presents some major advantages making it the most utilised tool to analyse gene expression. It represents a fast, high-throughput method allowing the study of a large number of samples with high sensitivity and reproducibility. However, the costs of the procedure in terms of required equipment, reagents, and chemicals remain significantly high. The sample preparation and loading for analysis is also quite time-consuming and the errors in the RNA/DNA extraction and reverse transcription can significantly impact and false the final result. Finally, the interpretation of the obtainable data is more complicated than in other techniques [42].

3.5.2 Alizarin Red S Staining

Extracellular mineralization is typically used as distinctive trait to recognise osteoblastic activity and maturation. The deposition of calcium in the ECM can highly impact the therapeutical potential of the investigated strategy, exploiting the osteoconductive properties of calcium compounds to trigger tissue regeneration and further cellular differentiation. For these reasons, the evaluation of novel approaches for bone repair frequently includes tools for the analysis of calcium deposition as indicator of the final stages of cell differentiation and matrix remodelling. In this context, the mostly used technique is Alizarin Red S staining (ARS), aiming to stain and detect the mineral content in the treated samples. The dye selectively binds to calcium producing an orange to red

pigment detectable with light microscopy or quantifiable measuring the sample absorbance typically at 405 nm. Thus, ARS represents an entry level and fast technique for the qualitative or quantitative analysis and comparison of mineralization in various setups and samples.

3.6 ELISA

The enzyme-linked immunosorbent assay (ELISA) is a biochemical assay based on the immobilization on a solid surface followed by a fluorescence-based measurement of the final concentration of the investigated reactant, typically a protein, antigen, or antibody [43]. The high sensitivity of the procedure relies on the specific binding of antigens to the respective capture antibody, allowing the detection of the target even at very low concentrations in the sample. The most commonly used setup is sandwich ELISA [44], showing superior specificity compared to the alternative options (direct or indirect ELISA). The analysis is typically performed in 96-well plates, coated with the specific antibody to immobilize the analysed reactant. The final detection is made possible with the addition and binding of a second antibody, labelled with an enzyme. The readout results from the interaction between the enzyme and a chromogenic substrate, producing a visible colour change or fluorescence necessary for the qualitative or quantitative measurement of the target concentration. The fluorescence-based detection offers a higher sensitivity for a more precise calibration and measurement.

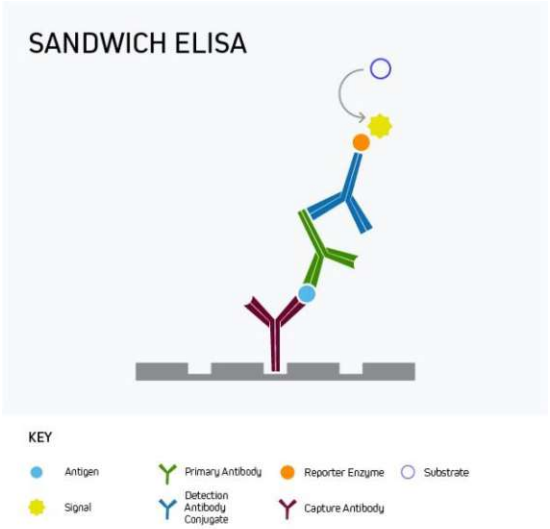

Figure 8: Sandwich ELISA format, with the binding of a capture and detection antibody for the detection of the target antigen. Adapted from [44].

The limits of ELISA are recognized in the possible occurrence of non-specific binding, leading to false positive readouts, or the colour change reaction proceeding indefinitely and thus producing an inaccurate measure over a longer period. Moreover, the preparation steps and incubation times make it a long procedure, despite the fast final measurement.
ELISA can be thus employed in various applications in biological assays, tracking the concentration of the desired molecule in the treated samples. In the current study, the outcomes of the performed release studies have been evaluated with ELISA to determine the amount of BMP-2 released over time and traceable in the supernatant collected from treated samples.

4 Materials and Methods

4.1 Ceramic Powder

The current study investigated the possibility to include calcium microparticles and BMP-2 in cell culture to enhance the achievable osteogenic differentiation. Moreover, similar ceramic materials have been utilized in literature for their binding affinity to proteins and growth factors, with BMP-2 being the most commonly exploited. Therefore, a release study was designed to determine the possibility to adsorb BMP-2 on micro-sized calcium particles.

4.1.1 Powder Preparation

A commercially available stock powder, provided by Kuros Biosciences (P21019), with a grain size of 45-63 µm, was processed to obtain a finer compound. Approximately 0.5 g were transferred in a mortar and manually ground with a pestle for 10 minutes to reduce the particles' size.
The particle size distribution before and after treatment was evaluated by image-based analysis. Images were taken by brightfield microscopy on a Zeiss LSM700. Images were analysed with ImageJ software. The finely ground powder was weighed in 10-15 mg aliquots into glass vials and heat sterilized at 160°C for 3 h, while the lids of the vials were UV sterilized for 30 min.

4.2 Scaffold

As previously introduced in section 3.2, a recently developed microscaffold [27] was used to encapsulate cellular spheroids and sustain their formation.
The microscaffold structure allows for further modification after printing. In this sense, a heparin functionalization was performed to improve the capability to bind BMP-2 and thus control its delivery in 3D culture. A two-step process was performed, including a first aminolysis followed by the coupling of a second compound, namely heparin. The latter was selected for its capability to bind a wide range of molecules and represents a cheap option in this sense. The resulting functionalization opened up new possibilities to merge the scaffolds advantages with other cues and agents.

4.2.1 Aminolysis

A batch of unmodified BBs, stored in tetrahydrofuran (THF), was transferred in a 250 mL round bottom flask, and washed with fresh THF. They were then resuspended in THF to a final concentration of 200 BBs/mL. In a beaker, a 1 eq. of a diamine (4,7,10-Trioxa-1,13-tridecanediamine, TTDA) and 0.5 eq. of a base (1,5-Diazabicyclo[4.3.0]non-5-ene, DBN) were dissolved in THF and the solution was stirred for 10 minutes at room temperature (RT) to obtain a homogeneous result. It was then added to the BBs suspension to reach a final concentration of 100 BBs/mL, and stirred for 45 minutes at RT. Once the stirring was stopped, BBs were left to precipitate for roughly 2 minutes before removing the solution and replacing it with the remaining amount for the second part of the aminolysis. The same procedure was repeated for a second time. Finally, BBs were washed once with fresh THF and three times with MES buffer (0.1 M at pH=5).

4.2.2 Heparin Coupling

The modification was continued with the heparin coupling using MES buffer as solvent. Two separate solutions were prepared using MES buffer (0.1 M) as solvent: a 0.4 mg/mL sodium heparin one, and a 0.1 M NHS + 0.01 M EDC-HCl solution. After complete dissolution via magnetic stirring, they were combined in a 1:1 ratio, and stirred once more for 15 minutes. The BBs were then resuspended in the coupling solution to a final concentration of 100 BBs/mL for 18 hours at RT and continuously stirred. Afterwards, the functionalized BBs were washed with distilled water. The amount of surface-bound heparin was measured using a commercially available Blyscan™ Blue GAG quantification kit (biocolor, B3000). Three replicates were sorted containing 100 modified BBs each in 1.5 Eppendorf tubes. 1 mL of dye reagent was added to each tube for 30 minutes, then they were centrifuged at 12000 rpm for 10 minutes. Supernatant was removed before adding 0.5 mL of dissociation reagent. Samples were vortexed and centrifuged for 3 minutes to remove any bubble. The resulting supernatant was transferred to a 96-well plate in duplicates, 0.2 mL each, and measured for absorbance at 656 nm along with standard solutions with known concentrations of dye reagent to derive a calibration curve.

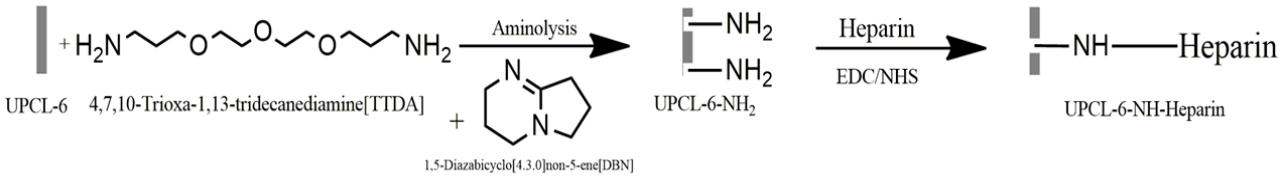

Figure 9: Two-step surface modification of BBs scaffolds.

4.3 BMP-2 Loading and Elution

4.3.1 Buckyballs

The heparinized BBs were sorted in three replicates containing 400 BBs/sample in 1.5 ml Eppendorf tubes. Then, 0.2 ml of a 0.5 µg/ml BMP-2 solution were added to each sample for the immobilization of BMP-2 onto the surface of UPCL-6 heparinized BBs. After 24 h incubation in a rotating system (Appligene Mini Hybridization Oven, Bimedis) at 37°C, the solution of BMP-2 was carefully removed, and the samples washed with fresh PBS to remove any loosely bound growth factor. Samples were treated with an elution buffer to release the BMP-2 bound to the respective substrates. Such buffer was composed of a 1% solution of Triton X-100, prepared using the diluent solution provided in the ELISA kit; 1 mL was added to each sample. After 40 minutes of incubation, the tubes were centrifuged 10 minutes at 10000 rpm, and the supernatant transferred in clean 1.5 mL Eppendorf tubes. The collected solutions were tested with ELISA to measure the eluted amount of BMP-2. The detected concentration was compared to the heparin content per BBs to establish the resulting binding ratio.

4.3.2 Ceramic Powder

A 1 mg/mL solution of CaP particles was prepared in PBS and three samples with 0.5 mL each were transferred into 1.5 mL Eppendorf tubes. The samples were centrifuged, the supernatant removed and 1 mL of a 100 ng/mL BMP-2 solution added. The samples were incubated for 24 h at 37°C in a

rotating system (Appligene Mini Hybridization Oven, Bimedis, USA) to avoid particle sedimentation. After the incubation, the samples were centrifuged at 10000xg for 10 min and the supernatant transferred into a new vessel. The loaded particles were washed once with 0.5 mL fresh PBS before centrifugation and removal of the solution. The supernatants of the incubation and washing solution were stored at -80°C until further analysis. The release study was started by the addition of 0.5 mL fresh PBS and the samples kept in motion using the rotation system. At defined time points, the samples were centrifuged, and the supernatant replaced with fresh PBS. All supernatants were stored at -80°C until further analysis.

4.3.3 ELISA Protocol

The analysis was performed using an ELISA kit (Peprotech, USA) according to the manufacturer SOP. In short, a 96-well plate was prepared with the addition of a blocking solution and incubated overnight. After washing the plate and removing the solution in excess, the BMP-2-specific capture antibody was added and incubated for 1 h. The same procedure was followed with the addition of samples (collected supernatants) and standards, and of the detection antibody, both followed by a 2 h incubation period at room temperature and subsequent washing step. Finally, the chromogenic substrate solution was added to trigger the reaction and color change for evaluation. The plate absorbance was measured with a microplate reader (Synergy H1 Microplate Reader, BioTek, USA) at 405 nm. A second readout was performed at 650 for wavelength correction due to plate-related aberrations.

4.4 MC3T3-E1 Culture

Different aspects of the interaction of MC3T3-E1 cells with BMP-2 and calcium microparticles were evaluated in our study, starting from the testing of BMP-2 potential a monolayer culture condition (2D) and continuing with the design of a 3D setup for the culture of scaffolded spheroids with CaP particles and BMP-2.

Cells were expanded at 37°C in 5% CO_2 in expansion medium, composed as follows:

- αMEM (Gibco 12571-063, 1000 mg/L glucose, 2 mM L-Glutamine);
- 10% (v/v) Newborn Calf Serum (NBCS, Sigma-Aldrich N4637);
- 1% (v/v) Penicillin/Streptomycin (P/S) solution, with a final concentration of 100 U/mL and 100 µg/mL, respectively.

4.4.1 2D Differentiation

After expansion, MC3T3-E1 cells at passage 6 were seeded in a 24-well plate in expansion medium at a concentration of 10000 cells/cm^2. An osteogenic medium (OM) was prepared to trigger cell differentiation as follows:

- Expansion Medium
- 50 µg/ml Ascorbic Acid
- 10 mM β-Glycerophosphate

When 100% confluency was reached, the medium was changed to start the study, comparing four different culture conditions, three biological replicates per group (Figure 10):

- Expansion media, as negative control group;
- OM, as positive control group;
- OM supplemented with BMP-2 at 100 ng/mL;
- OM supplemented with BMP-2 at 200 ng/mL.

Since previous studies suggested that the obtainable response could be increasing with growth factor dosage [29], two different concentrations were tested, namely 100 ng/mL (standard) and 200 ng/mL The day of media change (to OM or control media) was considered as day 0 for this specific experiment.

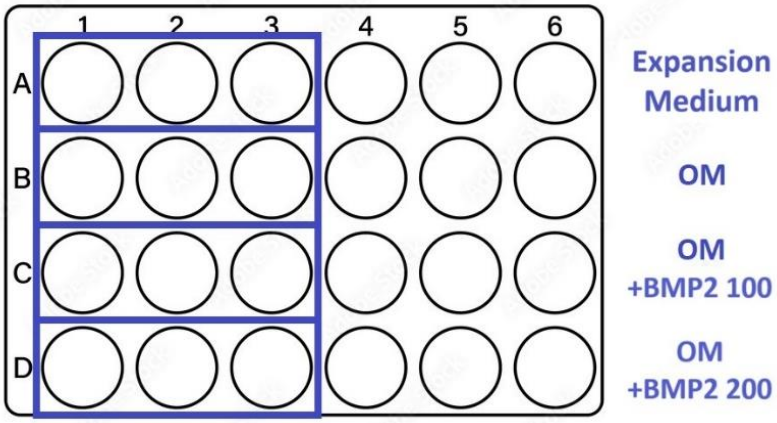

Figure 10: Seeding scheme for 2D differentiation.

Media were changed three times per week. Cells were cultured for 14 days and tested with Alizarin Red S (ARS) staining at day 7 and 14 to quantify the triggered mineral deposition.

4.4.2 Plate Coating

One of the available techniques to promote spheroids' formation is the utilization of low-binding or non-adherent surfaces in cultures.
A commercially available powder (amsbio [45]) was used for this specific purpose, allowing to coat culture plates and avoid cellular attachment. Lipidure® powder is a biocompatible and hydrophilic white powder which consists of 2-(methacryloyoxy)ethyl 2-(trimethylammonio)ethyl phosphate-n-butylmethacrylate copolymer. The building unit of this copolymer is 2-(methacryloyoxy)ethyl phosphorylcholine (MPC) monomer. Lipidure® mimics cell membrane surface and its molecular structure is the key for high hydrophilic nature and extremely low toxicity.
A 0.5% (w/v) solution was prepared in 100% ethanol (EtOH) diluting 50 mg of powder in 10 mL in a falcon tube. The obtained liquid was placed in water bath at 37°C for 1 hour to achieve complete dissolution. Then, 100 µL of solution were added to each well, removed after three minutes, and the plates were dried overnight and sterilized in UV light.

4.4.3 3D Differentiation

Once a significant difference was detected between treated and untreated samples, a similar procedure was performed also in three-dimensional conditions. Therefore, cells were transferred in low-adherent 96-well plates containing previously sorted microscaffolds (BBs) to promote spheroids' formation. In this case, two more conditions were investigated, incorporating calcium particles with or without BMP-2.

Therefore, the following cases were tested and compared in terms of cell differentiation and mineral deposition:

- Expansion medium, as negative control group;
- OM, as positive control group;
- OM with CaP particles' inclusion in cellular spheroids;
- OM with BMP-2-laden CaP particles' inclusion in cellular spheroids.

The same preparation and composition as in 2D culture were used for the two media (see section 4.4.1).

After expansion, MC3T3-E1 cells at passage 10 were resuspended in expansion medium and seeded in 96-well plates at a final concentration of 4000 cells/well in 100 µL of medium. The day of seeding was considered as day 0 for this experiment. The spare cell suspension was then frozen in QIAzol™ Lysis Reagent (Qiagen, 79306) and stored at -80°C for later evaluation with qPCR.

The calcium phosphate powder was resuspended in PBS and loaded with BMP-2 (for the last condition only) accordingly to the protocol previously presented in section 4.3.2. The obtained solution was then diluted and mixed with cell suspension to a final concentration of 0.1 mg/mL. 100 µL of such solution was transferred in each well, to obtain spheroids including 4000 cells and 10 µg of CaP per well.

Cell aggregation was monitored and documented with brightfield microscopy (LSM700, Zeiss, Germany), during the first three days of seeding. Once spheroids were fully formed, culture medium was substituted with the differentiation media for each condition.

Scaffolded spheroids were cultured over a 14 days period and tested at day 3 (start of differentiation), 10, and 17 with different techniques, described below, to measure mineral deposition and osteogenic markers' expression.

4.4 Alizarin Red S Staining

A 40 mM ARS solution was prepared by dissolving 684.5 mg of ARS powder (Sigma-Aldrich, A5533) in 50 mL of distilled water. The solution was then equilibrated with ammonium hydroxide (NH_4OH) and HCl to reach a pH of 4.2, sterile filtered, and stored in a tin foil-covered falcon tube at room temperature (RT).

Samples in a 24-well plate were washed twice with PBS and fixed with paraformaldehyde at 4% (ROTI®HistoFix) for 15 minutes at RT. Afterwards, the samples were washed three times with distilled water, and incubated at RT with 200 µL of ARS solution for 1 hour. Samples were washed five times with water and visualized with brightfield microscopy (LSM700, Zeiss, Germany).

Plates were incubated for 30 minutes at RT with 400 µL of a 10%. (v/v) acetic acid (Sigma-Aldrich, 320099) solution. The loosely attached cell layers were collected and transferred in fresh 1.5 mL Eppendorf tubes. The detached cells were vortexed, heated at 85°C for 10 minutes, cooled in ice for 5 minutes, and centrifuged at 20000xg for 15 minutes. The supernatant was collected and 350 µL were transferred into clean tubes. The samples were diluted with ammonium hydroxide to set acidic pH in the range of 4.1-4.5.

Standard ARS samples containing known concentrations of stain were prepared in parallel to calibrate the relating curve for comparison and interpretation of the obtained data. 10 mL of diluent were prepared with a 10% solution of acetic acid buffered at pH 4.3 with the addition of 10% ammonium hydroxide (Sigma-Aldrich, 320145). The stock solution at 40 mM was then diluted to a

2 mM concentration and a 1:2 serial dilution was performed to obtain the standard curve. The last point was represented by plain diluent at 0 mM (blank).
Afterwards, samples and standards were transferred in a 96-well plate in duplicates for evaluation, 150 µL per well, and their absorbance at 405 nm measured using the Synergy H1 Microplate Reader (BioTek, USA).
The resulting data were standardized subtracting the blank value, and the stain concentrations in the respective samples were derived from the trend line fitting the obtained standard curve. A dilution factor was introduced to compensate for the addition of NH_4OH for pH adjustment.
The same protocol can be also followed for samples cultured in 96-well plates, correcting all volumes by a factor of 0.375 and transferring 60 µL per well for final absorbance measurement.

4.5 Calcein Green Staining

To evaluate calcium deposition with Calcein Green staining, three spheroids per group were collected at each time point (days 3, 10 and 17 of culture), transferred in 1.5 mL Eppendorf tubes, and fixed for storage at 4°C until further analysis. After washing the samples with PBS, 1 mL of a 400 nM staining solution was added to each tube. The spheroids were incubated overnight at 37°C and washed with fresh PBS twice to remove the excess staining before imaging using confocal laser scanning microscopy (LSM800, Zeiss, Germany). For visualization, the excitation wavelength was set at 405 nm for the microscaffold and 488 nm for the Calcein Green stain, with the resultant emission measured in the ranges of 410-490 nm for the former case and 490-550 nm for BBs.

4.6 Polymerase Chain Reaction

30 spheroids were collected per group at each time point, transferred in fresh 1.5 mL Eppendorf tubes, and stored at -80°C in QIAzol™ Lysis Reagent (Qiagen, 79306) until further analysis.
In this case, the procedure focused on evaluating BGLAP and SPARC genes, encoding for osteocalcin and osteonectin, respectively. Both molecules are involved in matrix mineralization during the late stages of osteoblasts' differentiation. All data were calculated with respect to the expression of a housekeeping gene, in this case GAPDH, representative of the metabolic activity of the tested cells. Moreover, all groups were compared to the cell suspension frozen on the day of seeding, thus containing untreated spare cells from 2D culture. The delta-delta C_t method was used for comparison.

4.6.1 RNA Isolation

The analysis was started using an RNA isolation kit (RNeasy Plus Universal Mini Kit, Qiagen, Germany) according to the manufacturer SOP. Samples in Quiazol were disrupted with a micropestle before analysis to achieve complete cellular lysis. After adding 100 µL gDNA Eliminator Solution and 180 µL chloroform, tubes were centrifuged at 12000xg for 15 min at 4°C. The obtained aqueous phase was transferred to fresh microcentrifuge tubes. 70% ethanol was added, and the samples transferred into RNeasy Mini spin column, inserted in 2 mL collection tubes, before centrifuging for 15s at 8000xg at room temperature. The procedure was repeated another time, discarding the flow-through in between. 700 µL buffer RWT were added to the RNeasy spin column to wash the membrane, and centrifugation at 8000xg was performed for 15 s.

The flow-through was discarded before adding 500 µL buffer RPE and centrifuging the tubes for 2 min at 8000xg. The spin columns were placed in a new 1.5 mL collection tube, and 30 µL RNase-free water were added to elute the isolated RNA, which was collected in the tube with a 1 min centrifugation at 8000xg.
The obtained RNA concentration from each sample was measured with a Synergy H1 Microplate Reader (BioTek, USA). 2 µL samples were pipetted on the Take3 plate and absorbance was measured at 260 nm for RNA concentration, and at 280 nm for protein content. The 260/280 ratio represented an esteem of the samples' purity.

4.6.2 cDNA Synthesis

The measured RNA concentrations were used to calculate the amount of solution to mix with RNase-free water and 4 µL 5x All-In-One MasterMix (Applied Biological Materials Inc, Cat. No.G592) to obtain 100 ng of RNA in a 20 µL of reaction volume. The resulting mixtures were used for cDNA synthesis. After brief centrifugation and incubation at 25°C for 10 min, the prepared samples were incubated for 15 min at 42°C.

4.6.3 qPCR with SSoAdvanced SYBR Green Supermix

New reaction volumes were prepared for each sample and investigated gene. The selected target genes were BGLAP, SPARC, and GAPDH as housekeeping gene. All primers were purchased by Bio-Rad (USA).

Gene	name	assay ID
GAPDH	glyceraldehyde-3-phosphate dehydrogenase	qHsaCEP0041396
BGLAP	bone gamma-carboxyglutamate (gla) protein	qHsaCEP0041159
SPARC	secreted protein, acidic, cystein-rich (osteonectin)	qHsaCEP0057587

Table 1: List of primers utilized in qPCR.

Mastermix was prepared pipetting 10 µL SSoAdvanced Supermix, 2 µL sample cDNA, and 7 µL nuclease-free water per PCR reaction, including two extra volumes for safety. 20 µL of the prepared mix were transferred in fresh PCR strips in duplicates per sample and gene. The strips were then placed in the thermal cycler, properly closed with the respective lids, and the protocol shown in Table 2 below was applied.

qPCR step	temp.	time	**nr. of cycles**
Enzyme activation/initial DNA denaturation	95°C	30 sec	1 x
Denaturation	95°C	5 sec	40 x
Annealing/Extension	72°C	10 sec	
Melt Curve	65-95°C	2 sec/step	1 x

Table 2: Thermal cycling protocol used for qPCR analysis of the investigated genes.

The resulting C_q for the SPARC and BGLAP gene were confronted with the corresponding GAPDH one for each sample to calculate the delta value. Then, the delta-delta C_q ($\Delta\Delta C_q$) was obtained subtracting the delta value of the treated samples with the control group one. The final fold change in the gene expression was derived with the formula $2^{-\Delta\Delta Cq}$.
For comparison, all values were referred to the expression in cell suspension, frozen on the day of seeding, and thus set equal to 1.

5 Results

5.1 Ceramic Powder

A significant reduction in the average diameter, initially sitting in the range of 45-63 µm, can be noticed in Figure 11. The average particle size after grinding was 5.05 ± 0.615 µm (average ± SD), hence the manual processing produced roughly a 9-12-fold reduction.

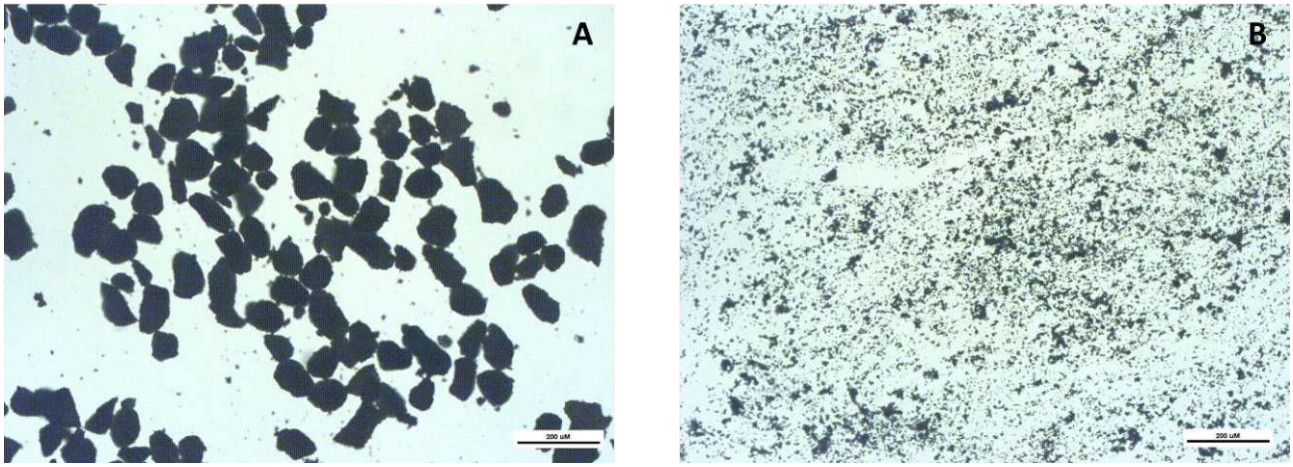

Figure 11: Grain size reduction before (A) and after (B) treatment via manual grinding.

Once these steps were completed, a release study was performed to assess the possibility to adsorb BMP-2 onto CaP particles, aiming to the subsequent inclusion in cellular spheroids similarly to the protocol used in Whitehead et al. study [22].

5.1.2 BMP-2 Release Study

The concentration in the collected supernatant was measured and used to calculate the total amount of released BMP-2 over time, as shown in the graph below (Figure 12).
The supernatant after incubation and following washing step accounted for 72.44 ± 18.98 pg in total. On the first day of release, 168.56 ± 43.13 pg were detected, while over 14 days the released amount was 422.54 ± 62.55 pg/mL, or 494.98 ± 65.37 pg adding the non-adsorbed portion. The detected BMP-2 concentration slightly decreased over time, producing the logarithmic-like pattern presented in Figure 12, with a value of about 50 pg recorded on the last two time points. Such findings supported the usage of CaP particles as loading substrates for BMP-2 delivery in 3D conditions.

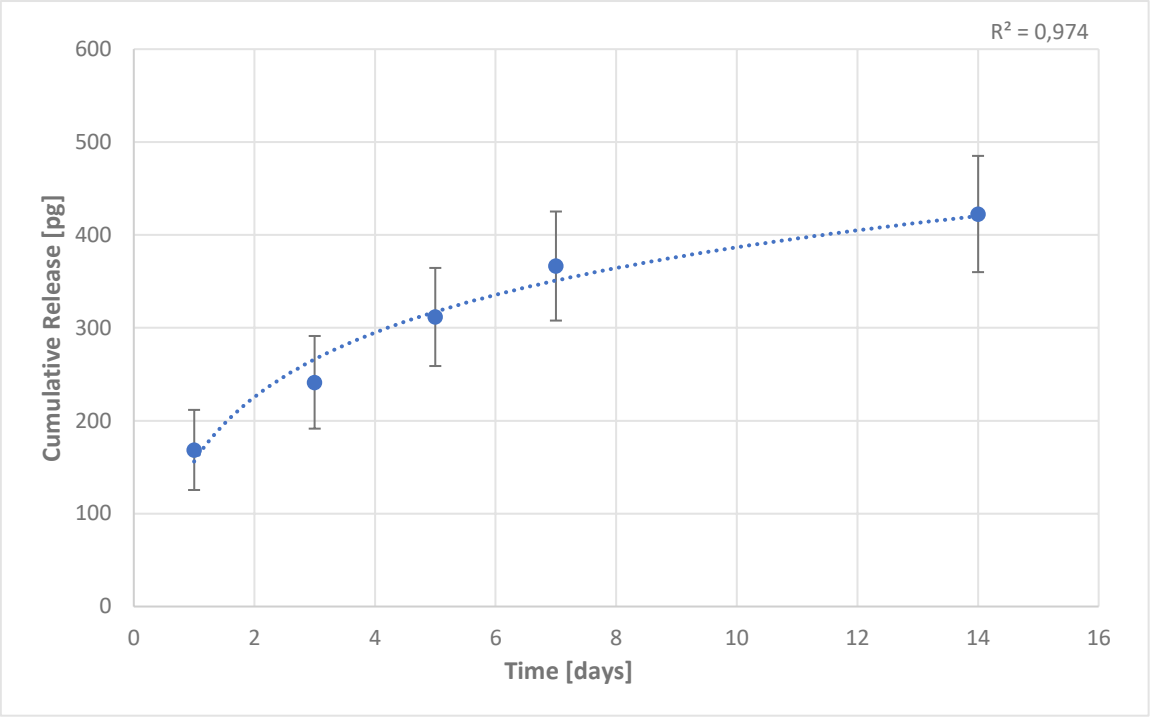

Figure 12: BMP-2 release in PBS over 14 days after 24 h incubation with calcium phosphate microparticles.

5.2 Scaffold

5.2.1 Surface Modification

The surface of the scaffolds was functionalized with heparin as described in Section 4.2.2. The resulting concentration was measured with a Blyscan™ Blue GAG quantification kit, assessing the amount of heparin bound to a single BB, as shown in Table 3.

	Heparin
µg/sample	2.61 ± 0.33
ng/BB	26.12 ± 3.27

Table 3: Measured heparin per sample and BB. Data expressed in mean ± SD.

5.2.2 BMP-2 Loading and Elution

The presence of heparin allows to bind diverse compounds to the scaffold's surface, in our case BMP-2. BBs were thus loaded with BMP-2 in a 24 hours-long incubation at 37°C, followed by a washing and elution step to measure the amount of bound growth factor. The procedure was performed in a duplicate to verify the repeatability and consistency of the protocol.

	Exp #1	Exp #2
pg/mL	1544.97 ± 70.95	1616.93 ± 250.71
pg/BB	3.86 ± 0.18	4.04 ± 0.63

Table 4: Eluted BMP-2 concentration in 1 mL Triton X-100 solution for 400 BBs.
The procedure was performed in a duplicate. Data expressed in mean ± SD.

A low binding ratio could be obtained with such a setup, sitting around 1:6000-7000, with 4 pg adsorbed on average per BB versus 26 ng of heparin in both attempts. Such findings required to

investigate an alternative option for the loading and integration of higher amounts of BMP-2 in spheroids.

5.3 MC3T3-E1 Culture

5.3.1 2D Differentiation

The first stage of MC3T3-E1 testing regarded 2D culture in four different conditions, namely standard culture in expansion medium, OM, and OM with the addition of BMP-2 at 100 and 200 ng/mL. Samples were evaluated with ARS staining after 7 and 14 days of differentiation, measuring their calcium content. Mineral deposition is typically used as an indicator of osteoblasts' activity and maturation.

Little to no mineralization was detected at day 7 for all groups, with comparable results for samples cultured in OM and OM supplemented with BMP-2. However, after two weeks of differentiation a much stronger response was obtained when BMP-2 was added to the osteogenic medium. As also shown in Figure 13, no stained calcium deposition was detected in the negative control group still, cultured in expansion medium only, thus presenting no changes with respect to the first time point. The second condition (OM) presented a little amount of calcium in the cellular monolayer as previously found on day 7. The BMP-2 [100] treated samples instead displayed a 20-fold difference in the second week in respect of the OM only control group, reaching a value of 394.43 ± 25.75 µM (versus 18.20 ± 0.82 µM). In respect to day 7, the 100 and 200 ng/mL BMP-2 groups registered a 10-fold and 15-fold increase, respectively.

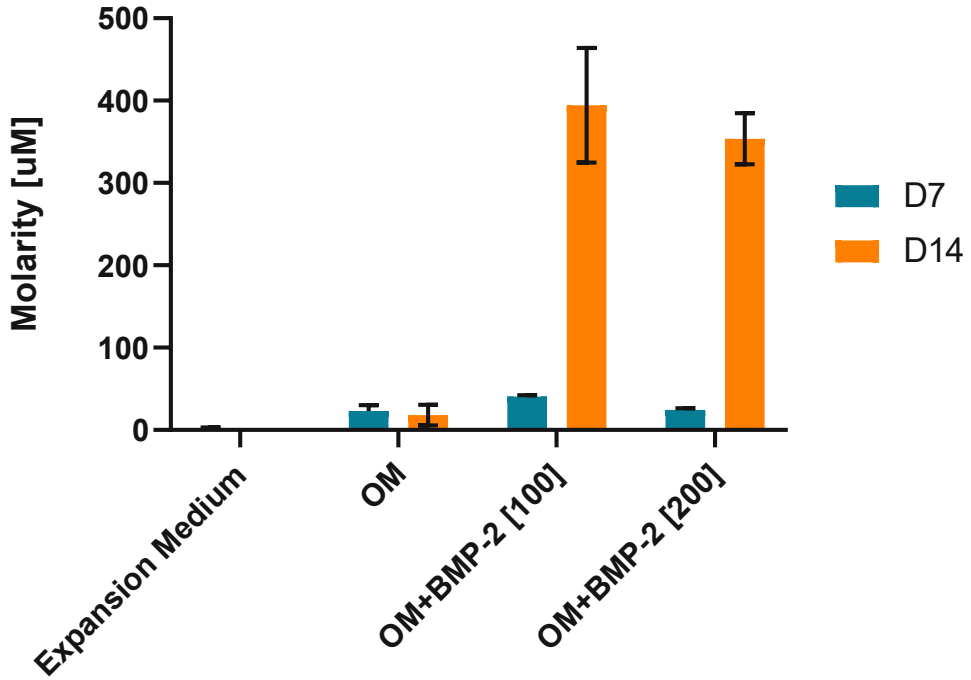

Figure 13: Stain molarity from ARS staining analysis after 7 and 14 days of differentiation, comparing 2D culture in expansion medium, OM, and OM supplemented with BMP-2 at 100 and 200 ng/mL.

A visual comparison is also presented in Figure 14, showing images of portions of the stained monolayers before detachment and subsequent elution for measurement.

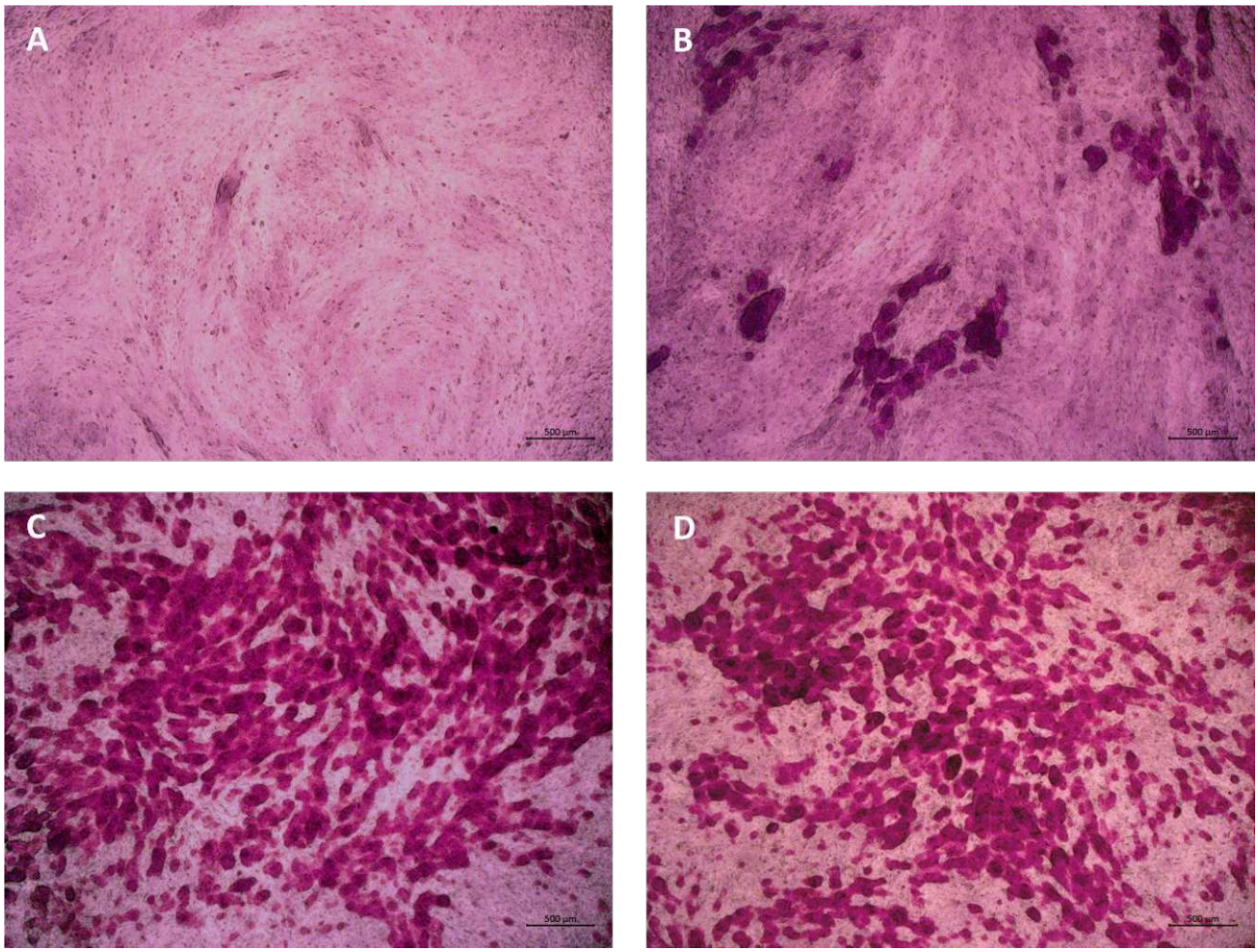

Figure 14: Detail of ARS staining in MC3T3-E1 2D culture for each group at day 14.
Images acquired with a LSM700 microscope (Zeiss, Germany).
A: Expansion medium; B: OM; C: OM + BMP-2 (100 ng/mL); D: OM + BMP-2 (200 ng/mL).

The control and BMP-2-supplied samples produced a visible difference in extracellular calcium amount and density, with the first ones having little to no stained areas. Treated groups instead were characterised by a much more consistent and homogeneous distribution in the well. The obtained findings, pointing out the strong sensitivity of MC3T3-E1 cells to BMP-2, confirmed the potential of such a lineage in bone-related studies. Thus, the following experiments focused on exploiting and measuring the extent of osteodifferentiation that can be triggered in a three-dimensional setup.

5.4 3D Differentiation

Spheroid formation was monitored after seeding to highlight the noticeable differences between cells-only and CaP-containing samples, while keeping all groups in expansion medium, using brightfield microscopy.

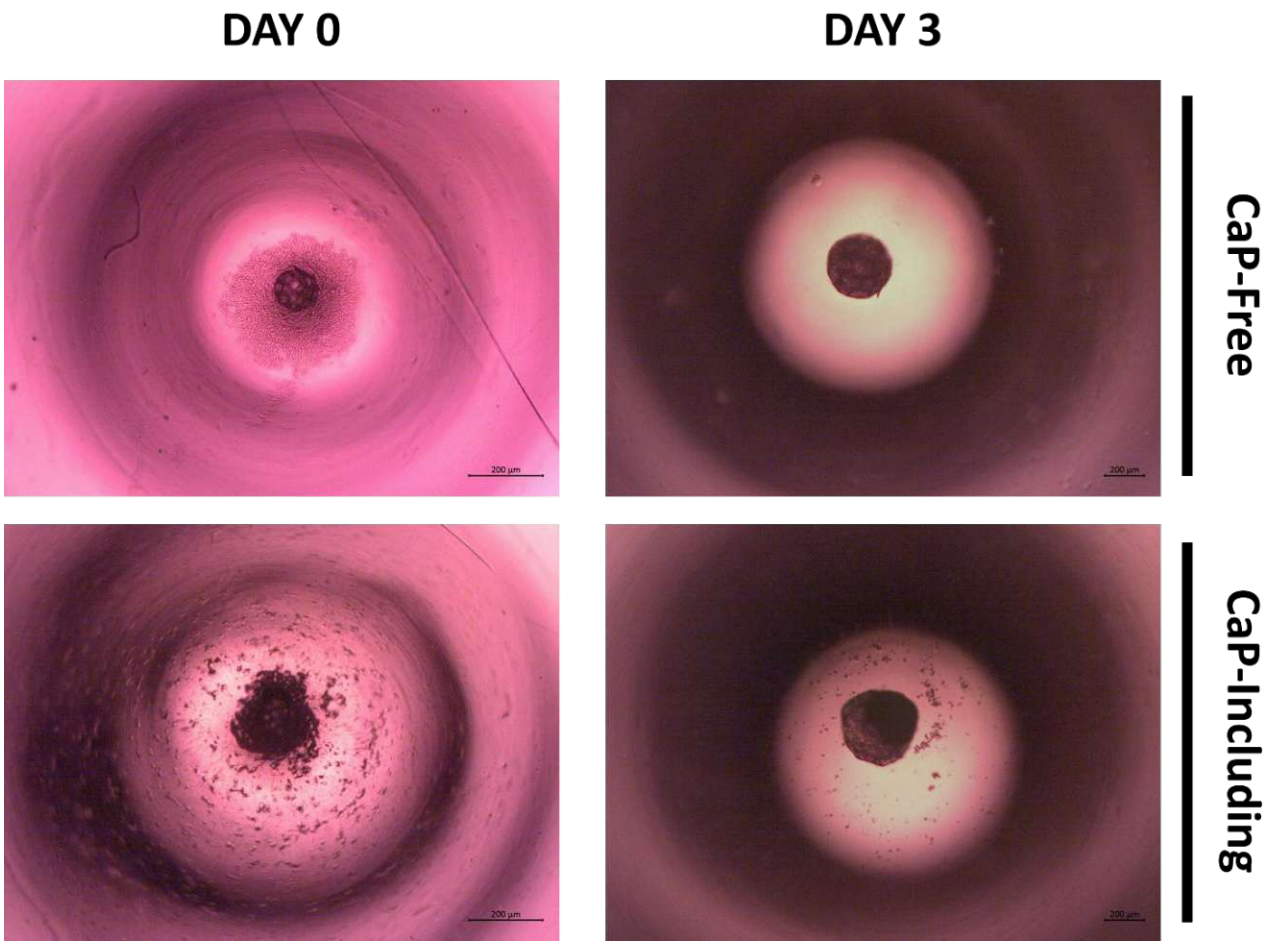

Figure 15: Cell distribution at day 0 after seeding in coated wells and at day 3 with spheroids fully formed, for calcium free (above) and including (below) groups.

Images taken after seeding showed a distinct pattern in the two groups: calcium grains seemed to gather at the bottom of the well faster than cells due to the significant difference in density. This first impression was confirmed after three days of culture, when spheroids were fully formed. Calcium grains compacted on one side of the spheroid (Figure 15, below), creating a denser mass, and thus no homogenous distribution was achieved. Such a characteristic was further investigated with other techniques, i.e. Calcein Green staining. On day 3, once all groups' spheroids were fully formed, expansion medium was substituted with OM for the last three groups to start the differentiation study.

5.4.1 Alizarin Red S Staining

Three scaffolded spheroids were used at each time point for ARS staining evaluation. The protocol was followed described in Section 4.4.

uM	D3	D10	D17
Expansion Medium	n.d.	n.d.	n.d.
OM	4.60 ± 0.36	n.d.	3.01 ± 0.28
CaP	17.08 ± 0.26	14.10 ± 0.13	13.85 ± 1.01
CaP+BMP-2	30.23 ± 0.29	6.41 ± 0.05	44.60 ± 0.07

Table 5: ARS staining molarity per sample for each group and time point. Data expressed in mean ± STD.

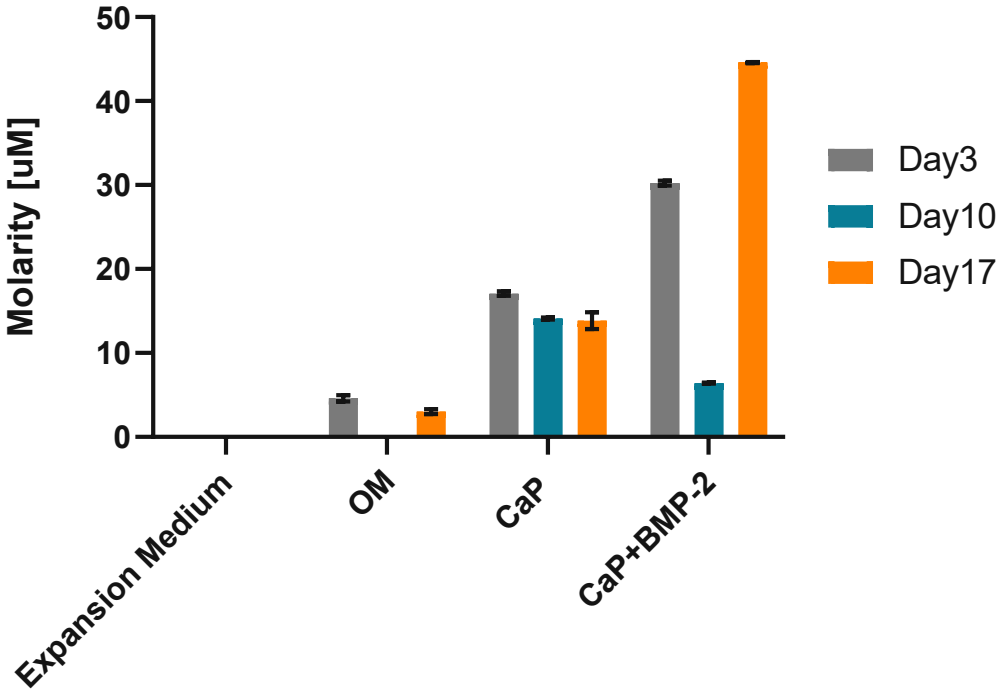

Figure 16: Stain molarity from ARS staining test in 3D culture.

No mineral content was detected in the first group, cultured in expansion medium, for all time points. OM produced little to no mineralization, with a maximum value of 4.60 ± 0.361 µM. Regarding the CaP-containing spheroids, two distinct trends were noticed. In the absence of BMP-2, the mineral content remained constant along the two weeks. The detected value at day 3 could thus be considered as the baseline for CaP-containing samples. The BMP-2-laden grains instead triggered extra deposition after 14 days, with the resulting stain molarity increasing from 30.23 ± 0.29 µM at day 3 to 44.60 ± 0.07 µM at day 17. Therefore, this latter group was the only one presenting an increase in staining molarity, confirming what found in 2D culture, with BMP-2 being able to promote mineralization while OM and CaP could not.

5.4.2 Calcein Green Staining

This technique allowed to stain calcium content in the tested samples and image it with laser scanning microscopy up to a certain depth within the spheroid (roughly 100 µm). Similarly to ARS, three samples were used per group and time point, and stained overnight at 37°C. Before visualization, they were washed twice with fresh PBS to remove of the excess staining.

Regarding the calcium-containing groups, the obtained images confirmed our first hypothesis on mineral distribution. After seeding, powder's grains collected and compacted before cells, forming one or more bulk masses. Such calcium aggregates seemed to remain unmodified until day 17 (2 weeks culture) when it resulted to be more homogenously and evenly spread all over the spheroids.

Contrary to our assumptions, some mineral deposition was detected also in both control groups at day 17, whether they had been cultured in expansion medium or OM. Such findings suggested that 3D culture's conditions alone could have triggered differentiation in MC3T3-E1 cells. However, the degree of mineralization was not enough to be detected with ARS staining as previously shown. Thus, further investigation was needed.

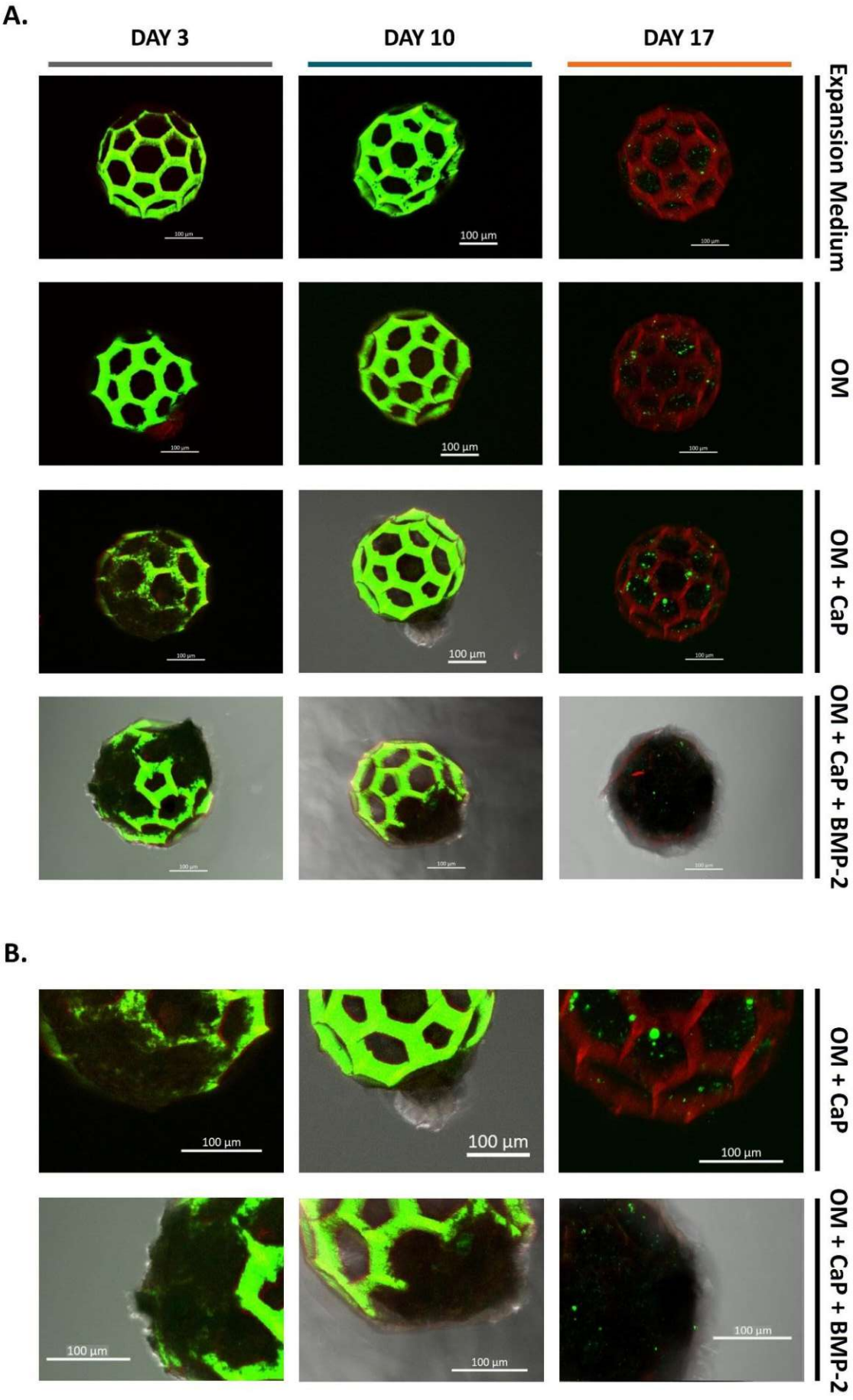

Figure 17: A-Calcein Green staining of mineral content and distribution of samples from each group and time point. B-Details of calcium-containing samples, showing mineral distribution and respective changes at different time points. Images acquired with LSM800 (Zeiss, Germany).

5.4.3 Polymerase Chain Reaction

qPCR represents the gold standard technique for the evaluation of gene expression in treated samples. In our case, two genes were selected, namely BGLAP and SPARC, encoding for osteocalcin and osteonectin, respectively. Both proteins are involved in the late stages of osteoblast maturation and extracellular mineralization. GAPDH was used as housekeeping gene for data analysis.

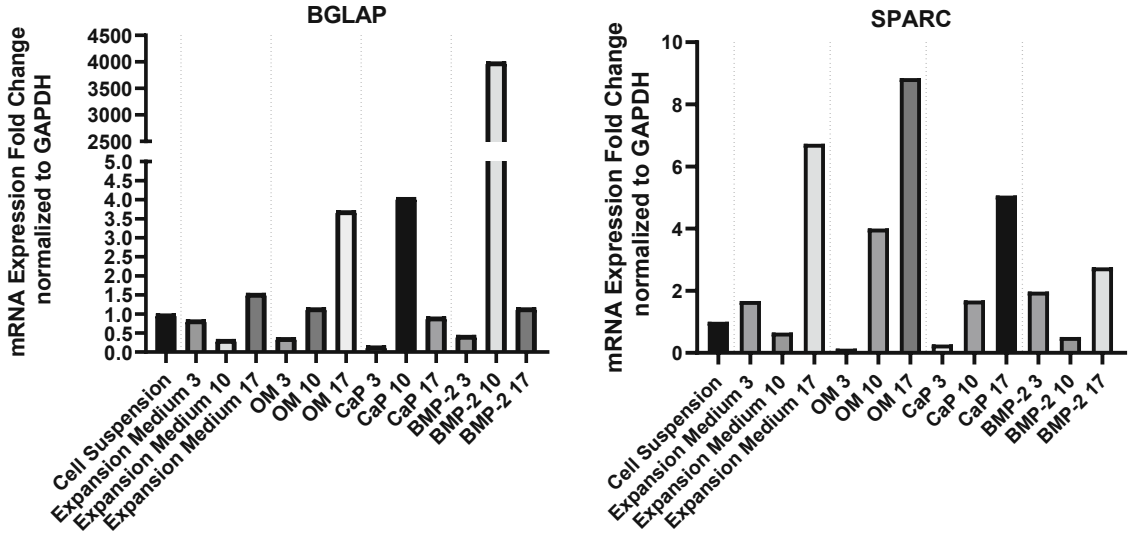

Figure 18: Fold change in expression of osteogenic markers' genes for each sample group and time point (corresponding day of culture indicated with the last digit).

Similarly to Calcein Green, qPCR data also suggested that MC3T3-E1 cells underwent differentiation in all tested conditions. Starting from the BGLAP gene, all groups presented downregulation at day 3, then two different trends were noticeable. In both control groups, gene expression increased from day 3 to 17, with a higher value for the OM one (3.71 versus 1.54). Calcium-containing samples instead showed a significant upregulation after only one week of differentiation, followed by a drop in the second week. In particular, the fold change reached a value of 3998 for BMP-2-including samples at day 10, a 1000 times difference in respect to the other conditions, a trend that could not be observed for the latter time point.

Regarding the SPARC gene, the fold change values increased from day 3 to 17 for all groups. In this case, the calcium-containing samples had the lower values, with the lowest corresponding to BMP-2 at day 17 (2.75). The largest upregulation was detected in the expansion medium and OM conditions, with the second one being the highest (8.85 versus 6.73). These findings can be connected to what was previously noticed in Calcein Green, with mineralization taking place in all groups. However, some markers' expression was triggered earlier with the addition of calcium particles and, most of all, BMP-2 as for BGLAP, leading to extra mineral deposition and remodelling.

6 Discussion

The main purpose of this study was to test different conditions, osteoinductive agents, and their combination to trigger osteodifferentiation in MC3T3-E1 cells. The overall procedure was divided into gradual steps: cell differentiation in 2D, evaluation of substrates for BMP-2 delivery, and subsequent inclusion of osteogenic cues in spheroids. In specific, it focused on evaluating the beneficial effects of incorporating BMP-2 and CaP particles in 3D culture, frequently used in literature due to their osteogenic potential.

MC3T3-E1 cells were tested in 2D conditions first, assessing the response to the addition of BMP-2 in the culture medium. Supposedly, such a lineage undergoes strong differentiation when exposed to high concentrations of BMP-2, thus the cells monolayers were cultured in OM supplemented with BMP-2 at 100 and 200 ng/mL. The control groups were cultured in expansion medium and OM only. Osteogenic differentiation was assessed using ARS staining to determine the amount of promoted mineral deposition.
After the first week of culture, no strong response was obtained, with minimal deposition in all conditions and no calcium content in the control group. The highest value corresponded to the samples supplied with BMP-2 at 100 ng/mL, almost doubling the OM and [200] ones. At day 14, no differences were noticed in the control groups (expansion medium and OM), while a 10-fold and 15-fold increase was registered for the [100] and [200] conditions, respectively, when compared to the previous time point. Also, a 20-fold difference was measured with respect to the OM group. Such findings confirmed that a strong differentiation can be obtained when exposing MC3T3-E1 cells to high doses of BMP-2. Contrary to the initial expectation, providing cells with a higher BMP-2 concentration (200 ng/mL versus 100 ng/mL) did not trigger a superior mineralization, but comparable values were obtained. Such results could be related to limitations of the used setup and procedure in terms of cell density and media volume per sample. Another possibility is having reached the highest achievable degree of mineralization already with 100 ng/mL.

A highly porous microscaffold was introduced in 3D culture, allowing better control on the final shape and geometry of cellular spheroids and the inclusion of other osteogenic factors in their formation, such as BMP-2 and CaP microparticles.
Two different options were tested for the delivery of BMP-2: binding to the microscaffold surface through the juxtaposition of heparin molecules, and adsorption onto calcium particles. Release studies were performed for both approaches. However, little to no BMP-2 was found in the supernatant using heparin as binding molecule. Therefore, a complete elution step was performed, using Triton X-100 as buffer. The obtained results have proven that a binding ratio to heparin of around 1:6000-7000 can be determined with this setup, corresponding to roughly 4 pg of BMP-2 bound to each BB (Table 4) against 25-27 ng of heparin. Such findings indicated that using heparin does not allow to load sufficient amounts of BMP-2 for our purposes and thus was not a suitable option.
Starting from the outcomes of previous studies carried out in our group, the calcium powder was manually ground with mortar and pestle to obtain a finer material with the average grain size, roughly 10-times smaller (Figure 11), and later sterilized, before application. The final powder was resuspended in a BMP-2 solution (100 ng/mL in PBS) and incubated for 24 hours at 37°C. Data from the release study onto calcium phosphate particles suggested that only a little amount of BMP-

2 was left in the supernatant after incubation. Almost all the growth factor added could be adsorbed onto the particles, but a deeper investigation is needed to confirm it. After 14 days of release, roughly 0.5 ng of BMP-2 was released. Therefore, BMP-2-laden CaP were introduced in 3D culture of spheroids.

The last experiment attempted to merge previous findings and exploit the potential of both BMP-2 and CaP powder in three-dimensional conditions. Cells were seeded in non-adherent 96-well plates with one microscaffold per well. The following conditions were tested: expansion medium, OM, or CaP particles with or without BMP-2. Cellular aggregation was followed and documented with brightfield microscopy in the first three days, as shown in Figure 15, to gain insight of CaP particles influence on spheroid formation. Then, spheroids were cultured for 14 days and the degree of differentiation at different time points was evaluated with ARS and Calcein Green staining, measuring mineralization, and qPCR.

By image analysis, it has been proven that CaP particles were sedimenting faster than cells, leading to inhomogeneous distribution of CaP in the final spheroids. The inorganic material was separated on one side of the spheroid with no significant remodeling found within one week of culture. After 14 days of differentiation, it appears that the distribution of CaP was changed towards a more homogeneous distribution. This could be caused by cell-driven remodeling of the matrix. Further deposition was detected in the BMP-2-treated group, as measured with ARS staining. For the other groups, the respective values remained constant at all time points. The higher starting value for the CaP-only samples corresponds to the initially included calcium amount. Calcein Green staining was used to get a deeper understanding of this process, verifying the final distribution of calcium within the samples. As expected, no mineral content was observed for the control groups (expansion medium and OM) within the first week of culture, However, some calcium deposition could be detected in such groups after two weeks of culture. On the other hand, the CaP-containing spheroids have confirmed the hypothesis on mineral remodeling, as CaP was found to be distributed evenly across the spheroids (Figure 17). Contrary to previous findings, obtained with ARS staining, the BMP-2-treated samples presented the least mineral deposition compared to the increased amount traceable in the other groups.

qPCR was also used to gain insights into the gene regulation during the progression of culture. Two genes were addressed and investigated, BGLAP and SPARC, encoding for osteocalcin and osteonectin, respectively. Both molecules are involved in calcium deposition and mineralization in the late stages of osteoblast maturation. The collected data have shown a similar trend in all groups for SPARC regulation, with an increased value after two weeks of differentiation. The gene's highest upregulation was detected in samples cultured in OM only, followed by expansion medium, CaP only and BMP-2-laden calcium particles. On the other hand, two distinct patterns could be recognized in BGLAP expression. The control groups have been shown to be upregulated only after two weeks, while calcium-containing groups have registered a significant increase already after one week. In particular, the BMP-2 treated spheroids have displayed a roughly 4000-fold change at day 10. A comparable result was reported by Koblenzer et al. [31], where plain OM was used for differentiation, with a major significant difference: such strong upregulation was reached after two weeks of culture, while in our case it was detected one week earlier.

These findings could also help us get through some of the processes governing differentiation and could be linked to previous results from Calcein Green and ARS staining. The earlier expression of BGLAP may be explaining two phenomena: firstly, the extra calcium deposition measured with

ARS, and secondly, together with the presence of osteonectin, the remodeling of calcium as noticeable in Calcein Green images, both taking place during the second week of culture, after the high peak in BGLAP upregulation. Further investigation was needed to gain major insight in the detection of differentiation in control groups too. Similar results can be found in literature, showing that the transition from 2D to three-dimensional culture conditions already triggers and initiates differentiation in MC3T3-E1, even when cultured in plain expansion medium [32]. qPCR data have shown that the investigated genes were upregulated after two weeks in 3D culture. The same occurred with OM without the involvement of BMP-2 or other additional growth factors, as already shown in analogous studies [31], [33]. However, the involvement of BMP-2 seemed to accelerate the differentiation process, stimulating further mineral deposition already at day 3, as detected by ARS staining, and major BGLAP upregulation after one week only.

7 Conclusion and Outlook

To conclude, the current study provided an evaluation of MC3T3-E1 lineage and its response to BMP-2, highlighting the obtainable strong response in terms of mineral deposition and differentiation. While in 2D, ARS staining was sufficient to show significant differences between control and treated samples, in 3D a wider and more complete evaluation was performed. BMP-2-triggered mineralization was shown in 2D culture samples with ARS. In the 3D case, ARS staining confirmed what was previously found in 2D, and Calcein Green staining provided a broader understanding of calcium distribution and its remodeling in the spheroids. Minor deposition was also detected in control groups, triggered by the transition to 3D culturing, even without the addition of further factors [32]. The achieved differentiation was further analyzed with qPCR to gain better insight into the gene expression. Although all groups showed different degrees of stimulation, the introduction of BMP-2-laden calcium microparticles during spheroid formation increased mineral deposition and expression of osteogenic markers.

The described results suggest that the usage of MC3T3-E1 cells may provide several benefits to the study and development of 3D-based bone models. The selected lineage was found to differentiate into osteoblasts in all conditions, from expansion medium to BMP-2-including media. The integration of CaP and BMP-2 in spheroid culture seems to accelerate such processes and trigger further mineralization and markers expression (e.g. BGLAP) earlier than the compared publications, where culture in non-supplemented OM was evaluated. To obtain a better comprehension of the osteogenic potential of MC3T3-E1, a broader screening could be performed with qPCR, measuring the expression of early markers (i.e. RUNX2, ALPL, Col1a1) alongside the late ones described in the present study. Further aspects of the cultured spheroids could be addressed, such as mechanical properties, cell viability, or histology.
Once the overall potential is determined in more detail, more complex constructs could be taken into consideration. The used microscaffold has been proven to allow the assembly of large-scale structures, via a bottom-up assembly, maintaining the previously described advantages in terms of control over the final shape and size [46]. Hence, the presented scaffold-based solution could be adapted and evolved with the involvement of MC3T3-E1 cells to design bone models for the study of available alternatives in the treatment of larger defects and various shapes.

Bibliography

[1] Y. Watanabe, N. Harada, K. Sato, S. Abe, K. Yamanaka, and T. Matushita, "Why bone tissue engineering with stem cells? Stem cell therapy: is there a future for reconstruction of large bone defects?," 2016.

[2] F. Schulze, A. Lang, J. Schoon, G. I. Wassilew, and J. Reichert, "Scaffold Guided Bone Regeneration for the Treatment of Large Segmental Defects in Long Bones," *Biomedicines*, vol. 11, no. 2. MDPI, Feb. 01, 2023. doi: 10.3390/biomedicines11020325.

[3] M. Filippi, G. Born, M. Chaaban, and A. Scherberich, "Natural Polymeric Scaffolds in Bone Regeneration," *Frontiers in Bioengineering and Biotechnology*, vol. 8. Frontiers Media S.A., May 21, 2020. doi: 10.3389/fbioe.2020.00474.

[4] E. Jimi, S. Hirata, K. Osawa, M. Terashita, C. Kitamura, and H. Fukushima, "The current and future therapies of bone regeneration to repair bone defects," *International Journal of Dentistry*. 2012. doi: 10.1155/2012/148261.

[5] L. C. Ingwersen, M. Frank, H. Naujokat, K. Loger, R. Bader, and A. Jonitz-Heincke, "BMP-2 Long-Term Stimulation of Human Pre-Osteoblasts Induces Osteogenic Differentiation and Promotes Transdifferentiation and Bone Remodeling Processes," *Int J Mol Sci*, vol. 23, no. 6, Mar. 2022, doi: 10.3390/ijms23063077.

[6] Y. Shuang, L. Yizhen, Y. Zhang, M. Fujioka-Kobayashi, A. Sculean, and R. J. Miron, "In vitro characterization of an osteoinductive biphasic calcium phosphate in combination with recombinant BMP2," *BMC Oral Health*, vol. 17, no. 1, Aug. 2016, doi: 10.1186/s12903-016-0263-3.

[7] R. Z. LeGeros, "Calcium phosphate-based osteoinductive materials," *Chemical Reviews*, vol. 108, no. 11. pp. 4742–4753, Nov. 2008. doi: 10.1021/cr800427g.

[8] R. Dwivedi *et al.*, "Polycaprolactone as biomaterial for bone scaffolds: Review of literature," *Journal of Oral Biology and Craniofacial Research*, vol. 10, no. 1. Elsevier B.V., pp. 381–388, Jan. 01, 2020. doi: 10.1016/j.jobcr.2019.10.003.

[9] A. M. Osyczka, D. L. Diefenderfer, G. Bhargave, and P. S. Leboy, "Different Effects of BMP-2 on Marrow Stromal Cells from Human and Rat Bone."

[10] B. E. Grottkau and Y. Lin, "Osteogenesis of Adipose-Derived Stem Cells," *Bone Research*, vol. 1. Sichuan University, pp. 133–145, Jun. 28, 2013. doi: 10.4248/BR201302003.

[11] H. Shafaei and H. Kalarestaghi, "Adipose-derived stem cells: An appropriate selection for osteogenic differentiation," *Journal of Cellular Physiology*, vol. 235, no. 11. Wiley-Liss Inc., pp. 8371–8386, Nov. 01, 2020. doi: 10.1002/jcp.29681.

[12] R. Liu *et al.*, "Myoblast sensitivity and fibroblast insensitivity to osteogenic conversion by BMP-2 correlates with the expression of Bmpr-1a," *BMC Musculoskelet Disord*, vol. 10, 2009, doi: 10.1186/1471-2474-10-51.

[13] E. Redondo-Castro, C. Cunningham, S. Cain, S. Allan, E. Pinteaux, and J. Miller, "Generation of Human Mesenchymal Stem Cell 3D Spheroids Using Low-binding Plates," *Bio Protoc*, vol. 8, no. 16, 2018, doi: 10.21769/bioprotoc.2968.

[14] K. H. Griffin, S. W. Fok, and J. Kent Leach, "Strategies to capitalize on cell spheroid therapeutic potential for tissue repair and disease modeling," *npj Regenerative Medicine*, vol. 7, no. 1. Nature Research, Dec. 01, 2022. doi: 10.1038/s41536-022-00266-z.

[15] T. Boix, J. Gómez-Morales, J. Torrent-Burgués, A. Monfort, P. Puigdomènech, and R. Rodríguez-Clemente, "Adsorption of recombinant human bone morphogenetic protein rhBMP-2m onto

hydroxyapatite," *J Inorg Biochem*, vol. 99, no. 5, pp. 1043–1050, 2005, doi: 10.1016/j.jinorgbio.2005.01.011.

[16] H. Autefage *et al.*, "Adsorption and release of BMP-2 on nanocrystalline apatite-coated and uncoated hydroxyapatite/β-tricalcium phosphate porous ceramics," *J Biomed Mater Res B Appl Biomater*, vol. 91, no. 2, pp. 706–715, Nov. 2009, doi: 10.1002/jbm.b.31447.

[17] Y. Li, T. Jiang, L. Zheng, and J. Zhao, "Osteogenic differentiation of mesenchymal stem cells (MSCs) induced by three calcium phosphate ceramic (CaP) powders: A comparative study," *Materials Science and Engineering C*, vol. 80, pp. 296–300, Nov. 2017, doi: 10.1016/j.msec.2017.05.145.

[18] X. Zhang, J. Guo, Y. Zhou, and G. Wu, "The roles of bone morphogenetic proteins and their signaling in the osteogenesis of adipose-derived stem cells," *Tissue Eng Part B Rev*, vol. 20, no. 1, pp. 84–92, Feb. 2014, doi: 10.1089/ten.teb.2013.0204.

[19] I. Song, B. S. Kim, C. S. Kim, and G. Il Im, "Effects of BMP-2 and vitamin D3 on the osteogenic differentiation of adipose stem cells," *Biochem Biophys Res Commun*, vol. 408, no. 1, pp. 126–131, Apr. 2011, doi: 10.1016/j.bbrc.2011.03.135.

[20] S. Gromolak, A. Krawczenko, A. Antończyk, K. Buczak, Z. Kiełbowicz, and A. Klimczak, "Biological characteristics and osteogenic differentiation of ovine bone marrow derived mesenchymal stem cells stimulated with FGF-2 and BMP-2," *Int J Mol Sci*, vol. 21, no. 24, pp. 1–22, Dec. 2020, doi: 10.3390/ijms21249726.

[21] L. D. Quarles, D. A. Yohay, L. W. Lever, R. Caton, and R. J. Wenstrup, "Distinct Proliferative and Differentiated Stages of Murine MC3T3-El Cells in Culture: An In Vitro Model of Osteoblast Development." [Online]. Available: https://academic.oup.com/jbmr/article/7/6/683/7500134

[22] J. Whitehead, A. Kothambawala, and J. Kent Leach, "Morphogen Delivery by Osteoconductive Nanoparticles Instructs Stromal Cell Spheroid Phenotype," *Adv Biosyst*, vol. 3, no. 12, Dec. 2019, doi: 10.1002/adbi.201900141.

[23] V. Agrawal and M. Sinha, "A review on carrier systems for bone morphogenetic protein-2," *J Biomed Mater Res B Appl Biomater*, vol. 105, no. 4, pp. 904–925, May 2017, doi: 10.1002/jbm.b.33599.

[24] N. E. Ryu, S. H. Lee, and H. Park, "Spheroid culture system methods and applications for mesenchymal stem cells," *Cells*, vol. 8, no. 12. MDPI, Dec. 01, 2019. doi: 10.3390/cells8121620.

[25] N. H. Lee, O. Bayaraa, Z. Zechu, and H. S. Kim, "Biomaterials-assisted spheroid engineering for regenerative therapy," *BMB Rep*, vol. 54, no. 7, pp. 356–367, 2021, doi: 10.5483/BMBRep.2021.54.7.059.

[26] N. V. Kosheleva *et al.*, "Cell spheroid fusion: beyond liquid drops model," *Sci Rep*, vol. 10, no. 1, Dec. 2020, doi: 10.1038/s41598-020-69540-8.

[27] O. Guillaume *et al.*, "Hybrid spheroid microscaffolds as modular tissue units to build macro-tissue assemblies for tissue engineering," *Acta Biomater*, vol. 165, pp. 72–85, Jul. 2023, doi: 10.1016/j.actbio.2022.03.010.

[28] C. A. Luppen, E. Smith, L. Spevak, A. L. Boskey, and B. Frenkel, "Bone Morphogenetic Protein-2 Restores Mineralization in Glucocorticoid-Inhibited MC3T3-E1 Osteoblast Cultures," *Journal of Bone and Mineral Research*, vol. 18, no. 7, pp. 1186–1197, Jul. 2003, doi: 10.1359/jbmr.2003.18.7.1186.

[29] S. L. Fung, X. Wu, J. P. Maceren, Y. Mao, and J. Kohn, "In vitro evaluation of recombinant bone morphogenetic protein-2 bioactivity for regenerative medicine," *Tissue Eng Part C Methods*, vol. 25, no. 9, pp. 553–559, Sep. 2019, doi: 10.1089/ten.tec.2019.0156.

[30] M. Izumiya *et al.*, "Evaluation of mc3t3-e1 cell osteogenesis in different cell culture media," *Int J Mol Sci*, vol. 22, no. 14, Jul. 2021, doi: 10.3390/ijms22147752.

[31] M. Koblenzer, M. Weiler, A. Fragoulis, S. Rütten, T. Pufe, and H. Jahr, "Physiological Mineralization during In Vitro Osteogenesis in a Biomimetic Spheroid Culture Model," *Cells*, vol. 11, no. 17, Sep. 2022, doi: 10.3390/cells11172702.

[32] J. Kim and T. Adachi, "Cell Condensation Triggers the Differentiation of Osteoblast Precursor Cells to Osteocyte-Like Cells," *Front Bioeng Biotechnol*, vol. 7, Oct. 2019, doi: 10.3389/fbioe.2019.00288.

[33] J. Kim, H. Kigami, and T. Adachi, "Comparative gene expression analysis for pre-osteoblast MC3T3-E1 cells under non-adhesive culture toward osteocyte differentiation," *J Biosci Bioeng*, vol. 132, no. 6, pp. 651–656, Dec. 2021, doi: 10.1016/j.jbiosc.2021.09.004.

[34] A. Arslan *et al.*, "Polymer architecture as key to unprecedented high-resolution 3D-printing performance: The case of biodegradable hexa-functional telechelic urethane-based poly-ε-caprolactone," *Materials Today*, vol. 44, pp. 25–39, Apr. 2021, doi: 10.1016/j.mattod.2020.10.005.

[35] M. R. Urist, "Bone: Formation by Autoinduction," *Science (1979)*, vol. 150, no. 3698, pp. 893–899, Nov. 1965, doi: 10.1126/science.150.3698.893.

[36] V. Rosen, "BMP2 signaling in bone development and repair," *Cytokine and Growth Factor Reviews*, vol. 20, no. 5–6. pp. 475–480, Oct. 2009. doi: 10.1016/j.cytogfr.2009.10.018.

[37] M. L. Zou *et al.*, "The Smad Dependent TGF-β and BMP Signaling Pathway in Bone Remodeling and Therapies," *Frontiers in Molecular Biosciences*, vol. 8. Frontiers Media S.A., May 05, 2021. doi: 10.3389/fmolb.2021.593310.

[38] V. Nguyen, C. A. Meyers, N. Yan, S. Agarwal, B. Levi, and A. W. James, "BMP-2-induced bone formation and neural inflammation," *Journal of Orthopaedics*, vol. 14, no. 2. Reed Elsevier India Pvt. Ltd., pp. 252–256, Jun. 01, 2017. doi: 10.1016/j.jor.2017.03.003.

[39] R. K. Saiki *et al.*, "Enzymatic Amplification of β-Globin Genomic Sequences and Restriction Site Analysis for Diagnosis of Sickle Cell Anemia," *Science (1979)*, vol. 230, no. 4732, pp. 1350–1354, Dec. 1985, doi: 10.1126/science.2999980.

[40] R. Higuchi, C. Fockler, G. Dollinger, and R. Watson, "Kinetic PCR Analysis: Real-time Monitoring of DNA Amplification Reactions," *Nat Biotechnol*, vol. 11, no. 9, pp. 1026–1030, Sep. 1993, doi: 10.1038/nbt0993-1026.

[41] K. Steward, "qPCR Analysis, How a qPCR Machine Works and qPCR Protocol." [Online]. Available: https://www.technologynetworks.com/analysis/articles/qpcr-analysis-how-a-qpcr-machine-works-and-qpcr-protocol-356835#:~:text=qPCR%20is%20a%20technique%20for,utilizing%20a%20DNA%20polymerase%20enzyme.

[42] Urška Čepin, "How Does qPCR Work? (Technology Basics)." [Online]. Available: https://biosistemika.com/blog/qpcr-technology-basics/

[43] S. D. Gan and K. R. Patel, "Enzyme immunoassay and enzyme-linked immunosorbent assay," *Journal of Investigative Dermatology*, vol. 133, no. 9, pp. 1–3, Sep. 2013, doi: 10.1038/jid.2013.287.

[44] M. Lewis, "Assay Setup: Sandwich ELISA for Allergy | 1," Aug. 2023. [Online]. Available: https://www.jacksonimmuno.com/secondary-antibody-resource/immuno-techniques/sandwich-elisa/

[45] "https://www.amsbio.com/lipidure-coat-plates/."

[46] G. Weisgrab *et al.*, "3D printing of large-scale and highly porous biodegradable tissue engineering scaffolds from poly(trimethylene-carbonate) using two-photon-polymerization," *Biofabrication*, vol. 12, no. 4, Oct. 2020, doi: 10.1088/1758-5090/abb539.